

**AN ARABIDOPSIS MADS-BOX GENE,
SEPALLATA 4, REGULATES FLOWERING TIME**

LIU JIE
(B.Sc., Shanghai Jiao Tong University)

**A THESIS SUBMITTED FOR
THE DEGREE OF MASTER OF SCIENCE**

DEPARTMENT OF BIOLOGICAL SCIENCES

NATIONAL UNIVERSITY OF SINGAPORE

2014

DECLARATION

I hereby declare that this thesis is my original work and it has been written by me in its entirety. I have duly acknowledged all the sources of information which have been used in the thesis.

This thesis has also not been submitted for any degree in any university previously.

Liu Jie

Liu Jie
1 JAN 2014

ACKNOWLEDGEMENTS

The overseas study experience in NUS is a precious gift in my life. I would like to acknowledge a lot of kind persons supporting me to go through this period and making this thesis possible.

First and foremost, I would like to express my sincere and heartfelt gratitude to my supervisor, Professor Yu Hao, for his professional guidance in every stage of my Master study and research, for his patience and impressive consideration when I encountered difficulties in my study and life, and for his sagacity enlightening me not only in my research but also in my daily life. Without his support, I could barely finish this thesis.

My sincere thanks also go to Dr. Liu Chang, Dr. Xi Wanyan and Dr. Hou Xingliang for their teachings and guidance in my project. Especially I am grateful to Dr. Liu Chang for his inspiration and advice on my research.

I also want to extend my special thanks to my dear lab members, Dr. Liu Lu, Dr. Shen Lisha, Dr. Wang Yue, Dr. Yan Yuanyuan, Dr. Thong Zhonghui, Dr. Gong Ximing, Norman Teo Zhiwei, Zhou Jiannan, Zhu Yang, Chen Ying, Li Chunying, Shen Qing, Dr. Ding Lihua, Dr. Song Shiyong, Dr. Chen Mingxun, Wang Yanwen, and Bao Shengjie, for their help and generously sharing their experience with me. Particularly, I would like to own my gratitude to my best friend and sister, Yuanyuan, for her company and encouragement when I felt down and when I was sick in this foreign country.

I would like to extremely thank the Department of Biological Sciences in NUS

Acknowledgements

for its financial support for my Master study with Research Scholarship.

Last but not least, I would like to give my special thanks to my beloved parents and sister. They are my spiritual support and support whatever decision I made. Finally, I feel grateful for all the good things and bad things happened on me, making me stronger and more mature.

January 2014

Liu Jie

TABLE OF CONTENTS

DECLARATION.....	i
ACKNOWLEDGEMENTS.....	ii
SUMMARY	vii
LIST OF TABLES	viii
LIST OF FIGURES	ix
LIST OF ABBREVIATIONS AND SYMBOLS	x
Chapter 1: Literature review	2
1.1 The floral transition is a crucial stage in plant life cycle	2
1.2 Flowering time is controlled by a complex network of five genetic pathways	5
1.2.1 The photoperiod pathway and the circadian clock.....	5
1.2.2 The vernalization and autonomous pathways	6
1.2.3 The gibberellin pathway	7
1.2.4 The age pathway	7
1.3 <i>SOC1</i> , an important flowering time integrator	8
1.4 <i>TEMPRANILLO</i> genes.....	9
1.5 <i>SEP4</i> functions in floral organ and meristem identity	11
1.6. Objectives of this study.....	14
Chapter 2: Materials and methods	16
2.1 Plant materials and growth conditions.....	16
2.2 Genotyping.....	16
2.2.1 Extraction of genomic DNA	16

2.2.2 Genotyping Polymerase Chain Reaction (PCR) amplification.....	17
2.3 Generation of transgenic plants	19
2.3.1 Construction of plasmid.....	19
2.3.2 Heat shock transformation	19
2.3.3 Colony PCR	19
2.3.4 Plasmid extraction and DNA sequencing analysis.....	20
2.3.5 Transformation into <i>Agrobacterium tumefaciens</i>	20
2.3.6 Floral dip.....	21
2.3.7 Selection of transgenic lines and genotyping.....	22
2.4 Expression analysis	22
2.4.1 Extraction of plant RNA	22
2.4.2 Reverse transcription	23
2.4.3 Quantitative real-time PCR.....	24
2.4.4 Semi-quantitative RT-PCR.....	26
2.5 Gus staining	28
2.6 Yeast two-hybrid assay (small scale)	30
2.6.1 Preparation of competent yeast cells.....	30
2.6.2 Transformation of competent yeast cells	31
2.7 Yeast two-hybrid screening using yeast mating.....	31
2.8 Chromatin Immunoprecipitation (ChIP) Assay	33
2.8.1 Nuclear fixation with formaldehyde	33
2.8.2 Nuclear protein-DNA extraction.....	34
2.8.3 Sonication and immunoprecipitation	34

2.8.4 DNA analysis	35
2.9 Transient expression in tobacco plants	38
Chapter 3: Results	40
3.1 Sequence analysis of <i>SEP4</i>	40
3.2 The <i>sep4-1</i> mutant shows indistinguishable phenotypes as wild-type, but overexpression of <i>SEP4</i> causes early flowering	42
3.3 Spatial and temporal expression patterns of <i>SEP4</i>	44
3.4 Subcellular localization of SEP4	47
3.5 Investigation of flowering genetic pathways that regulate <i>SEP4</i> expression	49
3.6 <i>sep4-1</i> single mutant enhances the late flowering phenotype of <i>soc1-2</i> ..	55
3.7 Identification of <i>SEP4</i> downstream genes	57
3.8 SOC1 and FUL are interaction partners of SEP4	65
3.9 Putative interacting partners of SEP4 explored by yeast two-hybrid screening	68
Chapter 4: Discussion	72
Chapter 5: Conclusion.....	78
References.....	80

SUMMARY

The timing of the transition from vegetative to reproductive phase in the model plant *Arabidopsis* is controlled by a complex regulatory network, which converges the environmental and endogenous signals on two floral pathway integrators, *FLOWERING LOCUS T* (*FT*) and *SUPPRESSOR OF OVEREXPRESSION OF CONSTANS1* (*SOC1*). *SOC1* is a member of the MADS-box family genes, some of which act as key flowering regulators in this network. Here we report that another MADS-box gene, *SEPALLATA 4* (*SEP4*), plays a redundant function with *SOC1* to promote flowering. *SEP4* has been found to be involved in floral organ development with other *SEP* homeotic genes. Unlike other *SEP* genes, which are expressed in the inflorescence tissues, *SEP4* is ubiquitously expressed in various plant tissues. Our studies show that *SEP4* expression is regulated by the autonomous and photoperiod pathways. Overexpression of *SEP4* causes early flowering, and *sep4-1* mutant enhances the late flowering phenotype of *soc1-2* mutant. Further work suggests that *FT* and two members of *RAV* (*RELATED TO ABI3* and *VPI*) family genes, *TEMPRANILLO1* (*TEM1*) and *TEM2*, are potential targets of *SEP4*. We are further characterizing the function of *SEP4* and its interacting proteins as well as downstream genes. These studies will shed light on the regulatory network involving *SEP4* in the control of flowering time in *Arabidopsis*.

LIST OF TABLES

Table 1. List of genotyping primers.	18
Table 2. List of quantitative real-time PCR primers	25
Table 3. List of semi-quantitative RT-PCR primers	27
Table 4. List of promoter regions primers	29
Table 5. List of ChIP assays primers.	37

LIST OF FIGURES

Figure 1. A regulatory network of the floral transition in <i>Arabidopsis</i>	4
Figure 2. Bioinformatic analysis of <i>SEP4</i> sequence.	41
Figure 3. <i>SEP4</i> regulates flowering time in <i>Arabidopsis</i>	43
Figure 4. Spatial expression patterns of <i>SEP4</i>	45
Figure 5. Temporal expression patterns of <i>SEP4</i>	46
Figure 6. Subcellular localization of GFP- <i>SEP4</i>	48
Figure 7. <i>SEP4</i> expression is affected by the autonomous pathway..	51
Figure 8. <i>SEP4</i> expression is not affected by the vernalization pathway.....	52
Figure 9. <i>SEP4</i> expression is not affected by the GA pathway..	53
Figure 10. <i>SEP4</i> expression is affected by the photoperiod pathway..	54
Figure 11. Loss of function of <i>SEP4</i> enhances the late-flowering phenotype of <i>soc1-2</i>	56
Figure 12. <i>FT</i> expression is regulated by <i>SEP4</i>	60
Figure 13. <i>TEM1</i> and <i>TEM2</i> expressions are upregulated in <i>soc1-2 sep4-1</i> plants.	61
Figure 14. <i>TEM1</i> expression is regulated by <i>SEP4</i>	62
Figure 15. Spatial expression patterns of <i>TEM2</i>	63
Figure 16. <i>SEP4</i> is directly associated with <i>TEM1</i> and <i>TEM2</i> chromatin. .	64
Figure 17. <i>SEP4</i> Interacts with <i>SOC1</i> and <i>FUL</i>	67
Figure 18. Putative interacting proteins of <i>SEP4</i> selected by yeast-two hybrid screening.	70
Figure 19. <i>In vivo</i> expression of <i>SEP4</i> fusion protein.	76

LIST OF ABBREVIATIONS AND SYMBOLS**Chemicals and reagents**

Basta	the herbicide glufosinate
dNTP	deoxynucleoside triphosphate
EDTA	Ethylene diamine tetraacetic acid
GA	gibberellin
GUS	β -glucuronidase
IPTG	isopropyl-beta-D-thiogalactopyranoside
KCl	potassium chloride
K_2HPO_4	dipotassium phosphate
KH_2PO_4	potassium phosphate (dibasic)
LB	Luria-Bertani medium
LiCl	lithium chloride
$MgCl_2$	magnesium chloride
MS	Murashige and Skoog medium
NaCl	sodium chloride
Na_2HPO_4	disodium phosphate
NaH_2PO_4	sodium phosphate (dibasic)
PEG	Polyethylene glycol
PMSF	phenylmethylsulfonyl fluoride
SDS	sodium dodecyl sulfate

List of abbreviations and symbols

Tris	hydroxymethyl-aminomethane
TAE	Tris acetate electrophoresis buffer
TE	Tris-EDTA
YPDA	yeast peptone dextrose adenine

Genes and proteins

<i>AP1</i>	<i>APETALA1</i>
<i>CAL</i>	<i>CAULIFLOWER</i>
<i>CO</i>	<i>CONSTANS</i>
FD	FLOWERING LOCUS D
<i>FLC</i>	<i>FLOWERING LOCUS C</i>
<i>FLD</i>	<i>FLOWERING LOCUS D</i>
<i>FLK</i>	<i>FLOWERING LOCUS K HOMOLOGY DO- MAIN</i>
<i>FRI</i>	<i>FRIGIDA</i>
<i>FT</i>	<i>FLOWERING LOCUS T</i>
<i>FUL</i>	<i>FRUITFULL</i>
<i>GA3OX1</i>	<i>GA 3-oxidase 1</i>
<i>GA3OX2</i>	<i>GA 3-oxidase 2</i>
GI	GIGANTEA
ING1	INHIBITOR OF GROWTH 1
<i>KNAT1</i>	<i>KNOTTED-LIKE FROM ARABIDOPSIS THALIANA 1</i>
<i>LD</i>	<i>LUMINIDEPENDENS</i>

List of abbreviations and symbols

<i>LFY</i>	<i>LEAFY</i>
MADS	MINICHROMOSOME, AGAMOUS, DEFICIENS, and SERUM RESPONSE FACTOR
<i>NGA1-4</i>	<i>NGATHA1-4</i>
<i>NGAL1-3</i>	<i>NGATHA-like 1-3</i>
PRC2	POLYCOMB REPRESSIVE COMPLEX2
<i>RAV</i>	<i>RELATED TO ABI3 and VP1</i>
<i>SEP1</i>	<i>SEPALLATA 1</i>
<i>SEP2</i>	<i>SEPALLATA 2</i>
<i>SEP3</i>	<i>SEPALLATA 3</i>
<i>SEP4</i>	<i>SEPALLATA 4</i>
<i>SMZ</i>	<i>SCHLAFMUTZE</i>
<i>SNZ</i>	<i>SCHNARCHZAPFEN</i>
<i>SOC1</i>	<i>SUPPRESSOR OF OVEREXPRESSION OF CONSTANS1</i>
<i>SPL</i>	<i>SQUAMOSA PROMOTER BINDING PRO- TEIN-LIKE</i>
<i>SUC2</i>	<i>SUCROSE-PROTON SYMPORTER 2</i>
SVP	SHORT VEGETATIVE PHASE
<i>TEM1</i>	<i>TEMPRANILLO1</i>
<i>TEM2</i>	<i>TEMPRANILLO2</i>
<i>TFL1</i>	<i>TERMINAL FLOWER 1</i>

List of abbreviations and symbols

<i>TOE1</i>	<i>TARGET OF EAT 1</i>
<i>TOE2</i>	<i>TARGET OF EAT 2</i>
<i>TSF</i>	<i>TWIN SISTER OF FT</i>
<i>TUB 2</i>	<i>TUBULIN2</i>
VIN3	VERNALIZATION INSENSITIVE 3
VP1	VIVIPAROUS1
VRN2	VERNALIZATION 2
WOX13	WUSCHEL-RELATED HOMEBOX 13

Units and measurements

bp	base pairs
°C	degree Celsius
d	day
g	centrifugal force
g	gram
h	hour
l	litre
kb	kilo base-pairs
kDa	kilo Dalton
M	molar
min	minute
ml	mililitre
mM	milimolar
ng	nanogram

List of abbreviations and symbols

OD	optical density
rpm	revolutions per minute
sec	second
U	unit
w/v	weight per volume
µg	microgram
µl	microlitre
µM	micromolar

Others

CaMV	cauliflower mosaic virus
cDNA	complementary deoxyribonucleic acid
Col	Columbia
DNA	deoxyribonucleic acid
mRNA	messenger ribonucleic acid
PCR	polymerase chain reaction
RT-PCR	reverse transcription polymerase chain reaction
pH	potential of hydrogen
SAM	shoot apical meristem
T-DNA	transfer DNA
UTR	untranslated region
SDS-PAGE	SDS Polyacrylamide Gel Electrophoresis

CHAPTER 1:

LITERATURE REVIEW

Chapter 1: Literature review

1.1 The floral transition is a crucial stage in plant life cycle

The life cycle of almost all flowering plants can be divided into two major developmental stages, the embryonic and the post-embryonic stages. During the embryogenesis, an embryonic shoot apical meristem (SAM) is established. After the germination, the post-embryonic stage begins and the SAM gives rise to all the organs of the aerial part except cotyledons (Fosket, 1994; Hamada et al., 2000). In the model plant *Arabidopsis thaliana*, the vegetative and the reproductive phases are the two morphologically and physiologically distinct phases during the post-embryonic development. At the vegetative phase, the vegetative SAM generates vegetative tissues, such as leaves. This phase can be further divided into the juvenile phase and the adult phase, which can be distinguished by the density of trichomes on the leaf surface (Chien and Sussex, 1996; Telfer et al., 1997). During the floral transition, the vegetative SAM is transformed into the inflorescence meristem (IM) that produces floral meristems (FM) on its flank during the reproductive development.

In order to maximize reproductive success and seed production, the timing of floral transition is tightly controlled by environmental and endogenous signals. The genetic control of flowering time of *Arabidopsis* has been extensively investigated as it is a typical experimental model as an angiosperm plant (Meyerowitz and Somerville, 1994). A complex genetic regulatory network containing a large number of flowering time regulators has been established. Most of these genes function in five major genetic pathways in response to various environmental and developmental signals (Baldev and Lang, 1965;

Bernier, 1988; Napp-Zinn and Atherton, 1987; Srikanth and Schmid, 2011). Flowering, in response to the environmental changes, is mainly controlled by the photoperiod and vernalization pathways, while other three pathways, namely the autonomous, gibberellins, and age-dependent pathways are influenced by the endogenous cues. The flowering signals perceived from these five genetic pathways converge to regulate some floral pathway integrators, which in turn, govern the switch from the vegetative to the reproductive growth (Fornara et al., 2010) (Figure 1).

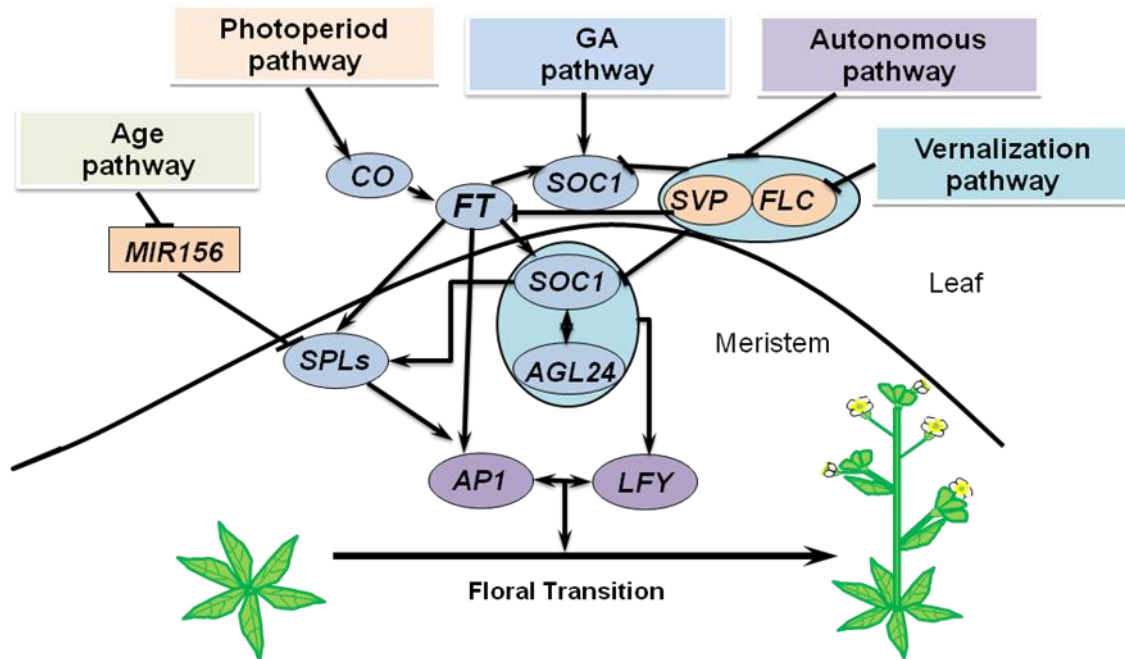


Figure 1. A regulatory network of the floral transition in *Arabidopsis*.

The timing of the floral transition is tightly controlled by an intricate network of multiple genetic pathways. The five genetic pathways integrate the environmental and developmental signals into the floral integrators, *FT* (*FLOWERING LOCUS T*) and *SOC1* (*SUPPRESSOR OF OVEREXPRESSION OF CONSTANS1*). The FLC-SVP complex represses *SOC1* and *FT* expression. The FT-FD complex promotes the expression of *SOC1* and *AP1*. These integrators further activate *LFY* and other floral meristem identity genes, such as *AP1*. Therefore, the floral transition is initiated by producing the floral meristems instead of leaves from the apical meristem.

1.2 Flowering time is controlled by a complex network of five genetic pathways

1.2.1 The photoperiod pathway and the circadian clock

In *Arabidopsis*, flowering is promoted in long summer days, while repressed in short winter days. The photoperiod pathway promotes flowering in response to the long day conditions. The light signals are perceived in leaves and then transmitted to the SAM to promote the transition from the vegetative SAM to the IM. This process is mediated by the movement of the so-called “florigen”, *FLOWERING LOCUS T* (*FT*), and its homolog *TWIN SISTER OF FT* (*TSF*) (Kobayashi and Weigel, 2007; Turck et al., 2008). *FT* and *TSF* are small proteins that serve as mobile signals moving from leaves to the SAM. At the SAM, these two proteins interact with *FLOWERING LOCUS D* (*FD*), a bZIP transcription factor. The heterodimer activates some downstream targets, such as *APETALA1* (*API*), *SUPPRESSOR OF OVEREXPRESSION OF CONSTANS1* (*SOC1*) and *FRUITFULL* (*FUL*) at the SAM. These three MADS-box transcription factors are among the earliest genes to be activated after exposure to LDs (Lee et al., 2000; Putterill et al., 2004; Simon et al., 1996).

Activation of *FT* and *TSF* in response to LDs requires a central regulator *CONSTANS* (*CO*) in the photoperiod pathway, which encodes a zinc finger protein. During LDs, light can promote the interaction between *GIGANTEA* (*GI*) and a family of F-box ubiquitin ligases. The stable F-box proteins degrade a set of transcription repressors of *CO*, thus promoting *CO* expression. The up-regulation of *FT* by *CO* in LDs is precisely controlled by light stimuli and the internal circadian clock signals. The circadian clock ensures that the transcription of *CO* is cyclically expressed with a broad bi-phasic peak in long days

and a slightly narrower peak in short days. And *GI* enhances this peak under LDs (Dunlap, 1996; Kay and Millar, 1995). In LDs, the high amount of *CO* mRNA appears coincides with the light at dawn and afternoon to induce flowering. However, in SDs (Short Days), high levels of *CO* occur in the dark. Without the correlation of *CO* and light, *FT* expression cannot be up-regulated, which leads to the delay of flowering (Putterill et al., 2004; Samach et al., 2000).

1.2.2 The vernalization and autonomous pathways

Vernalization is a prolonged cold treatment, which mimics the winter condition, to promote flowering. This strategy contributes to preventing improper flowering during autumn and winter (Napp-Zinn, 1961). Recent genetic analyses have shown that natural alleles of two genes, *FLOWERING LOCUS C (FLC)* and *FRIGIDA (FRI)*, respond to the vernalization. *FLC* encodes a MADS-box transcription factor that acts as a repressor of flowering. In the leaves, *FLC* represses the expression of *FT* and another two flowering activators, *FD* and *SOC1* (Lee et al., 2000; Michaels and Amasino, 1999), while in the shoot apex, *FLC* interacts with another flowering suppressor, *SHORT VEGETATIVE PHASE (SVP)*, and this protein complex suppresses *SOC1* expression through directly binding to a specific sequence (CArG box) in its promoters (Li et al., 2008). In winter annuals of *Arabidopsis*, vernalization reduces the expression of *FLC* and maintains its expression at low levels when the plants are back to warm conditions. This process involves the PHD finger protein *VERNALIZATION INSENSITIVE 3 (VIN3)* and a *POLYCOMB REPRESSIVE COMPLEX2 (PRC2)* including *VERNALIZATION 2 (VRN2)* (Sung and Amasino, 2004a; Sung and Amasino, 2004b). Downregulation of *FLC* enables partial derepression of the florigen gene, *FT*, in the leaf, and also allows the meri-

stem to acquire the competence to respond to *FT* (Samach et al., 2000; Searle, 2006).

Besides the environmental factors, some internal signals also regulate flowering. The autonomous pathway responds to the endogenous signals such as leaf number and size. A group of genes including *FCA*, *FY*, *FLOWERING LOCUS D (FLD)*, *FVE*, *FPA*, *LUMINIDEPENDENS (LD)* and *FLOWERING LOCUS K HOMOLOGY DOMAIN (FLK)*, is involved in this pathway (Koornneef et al., 1991). When any of these genes is mutated, the plants show late-flowering phenotype both in LDs and SDs. The major target of these genes in the autonomous pathway is *FLC*, which is highly expressed in the mutants of autonomous pathway. In conclusion, genes of the autonomous pathway promote flowering by repressing *FLC* expression (Koornneef et al., 1991; Michaels and Amasino, 2001).

1.2.3 The gibberellin pathway

Bioactive gibberellins (GAs) are plant hormones controlling growth and developmental processes such as seed germination, stem growth, floral transition, and flower development (Swain and Olszewski, 1996). The GA-deficient mutant *gal-3* fails to flower in SDs, while the application of exogenous GA accelerates flowering of wild-type plants under short day conditions (Koornneef et al., 1985; Sun and Kamiya, 1994; Wilson et al., 1992). These observations suggest that GA accelerates flowering under SDs. It has been shown that GA effects on flowering is mediated by two DELLA proteins, RGA and GAI, in the GA signaling pathway (Dill et al., 2001). However, how these DELLA proteins regulate other flowering time genes are so far largely unknown.

1.2.4 The age pathway

miR156 and its targets, the *SQUAMOSA PROMOTER BINDING PROTEIN-LIKE*

(*SPL*) transcription factors, constitute the age pathway responding to the endogenous signals (Wang et al., 2009; Wu et al., 2009). In *Arabidopsis* and maize, miR156 represses *SPLs* in the SAM to repress flowering. As the plants age, the expression of miR156 is down-regulated. Consequently, the suppression of *SPLs* is released and thus the floral transition is promoted at the proper age even without inductive photoperiod signals under SDs. In *Arabidopsis*, there are two broad groups of miR156-regulated *SPLs*. *SPL3*, *SPL4*, and *SPL5* encode small proteins mainly containing the SBP DNA-binding domain, while the other eight *SPLs* encode bigger proteins, including *SPL9* and its paralog *SPL15*, which affect the leaf initiation rate (Wang et al., 2009). Moreover, recent studies have shown that the first group of *SPLs* is not only influenced by the age pathway, but also regulated by *FT* in the photoperiod pathway and affected by the GA pathway through a *SOCI*-dependent mechanism (Jung et al., 2012).

1.3 *SOCI*, an important flowering time integrator

The various flowering time pathways function cooperatively to form a complex flowering regulatory network and they ultimately coverage on the regulation of several floral pathway integrators, including *FT*, *SOCI* and *LEAFY* (*LFY*) (Putterill et al., 2004; Simpson and Dean, 2002). These integrators further activate *LFY* and other floral meristem identity genes, such as *APETALA1* (*API*) and *CAULIFLOWER* (*CAL*), which initiate the production of floral meristems (FMs) instead of leaves from the apical meristem.

SOCI encodes a MADS-box protein and was first isolated in the screening of suppressors of overexpression of *CO* (Lee et al., 2000). Loss of function of *SOCI* greatly suppresses the early flowering phenotype of *35S:CO*, and *SOCI* has also been suggested as an immediate target of *CO* (Suárez-López et al., 2001). *SOCI* is regulated by the photo-

period pathway, age pathway and gibberellin pathway. In the photoperiod pathway, *CO* regulates *SOC1* through *FT* (Yoo, 2005). *SOC1* expression level is increased in *35S:FT* and decreased in the *ft* mutant (Wigge et al., 2005; Yoo, 2005). Furthermore, *SOC1* was found to interact with *AGL24* and they positively regulate each other's expression to integrate the flowering signals (Liu et al., 2008). Upregulation of *SOC1* in the meristems is one of the earliest events in the floral transition under the photoperiod pathway. Additionally, previous studies showed that *SOC1* regulates *FT* expression by directly repressing some AP2-like flowering repressors including *TARGET OF EAT 1 (TOE1)*, *TOE2*, *SCHLAFMUTZE (SMZ)*, *SCHNARCHZAPFEN (SNZ)*, *TEMPRANILLO 1 (TEM1)* and *TEM2*. These repressors repress *FT* expression to prevent precocious flowering (Castillejo and Pelaz, 2008; Jung et al., 2012; Mathieu et al., 2009). In a genome-wide ChIP-chip (Chromatin immunoprecipitation followed by hybridization to whole-genome tiling arrays) analysis, these AP2-like repressors including *TOE1*, *TOE3*, *SMZ*, *TEM1* and *TEM2* were downregulated by *SOC1*, and *SOC1* directly bind to their CArG-box motifs (Tao et al., 2012).

In the age-dependent pathway, *SOC1* is regulated by the *SPL* transcription factors whose expression levels are increased during plant growth. For instance, *SPL9* directly binds to the first intron of *SOC1* (Wang et al., 2009). On the other hand, *SOC1* directly binds to the promoters of *SPL3*, *SPL4* and *SPL5* to form a positive feedback loop. The *SOC1-SPL* pathway also perceive GA signals to promote flowering under SD conditions (Jung et al., 2012).

1.4 *TEMPRANILLO* genes

TEM1 and *TEM2* belong to the *RAV (RELATED TO ABI3 and VPI)* family which con-

sists of at least 13 members in *Arabidopsis* (Swaminathan et al., 2008). *RAV1*, *RAV2/TEM2*, *TEM1*, *NGATHA1-4(NGA1-4)*, and *NGATHA-like 1-3 (NGALI-3)* belong to this transcriptional factors family and they are involved in development and physiology in plants (Swaminathan et al., 2008). *RAV1* and *TEM2* were initially identified as homolog to the maize *VIVIPAROUS1 (VP1)* based on the B3 DNA-binding domain (Kagaya et al., 1999). In addition to the B3 domain, *TEM1*, *TEM2* and other four *RAV* members contain an AP2/ERF domain, which is also a DNA-binding domain (Kagaya et al., 1999).

In *Arabidopsis*, *TEM1* and *TEM2* have been shown to act redundantly to link the photoperiod pathway and the GA pathway in regulating flowering (Castillejo and Pelaz, 2008; Osnato et al., 2012). RNAi-*tem1/2* and *tem1-1 tem2-2* double mutants flower earlier than wild-type, whereas overexpression of *TEM1* and *TEM2* plants show extremely late-flowering under LD conditions (Castillejo and Pelaz, 2008; Osnato et al., 2012). Several evidences suggest that *TEM1* and *TEM2* function as repressors of the floral transition to directly bind to a consensus bipartite sequence element in the 5'untranslated region (UTR) of *FT*. The binding site is located right beside the putative binding site for the activator complex consisted of CO and the CCAAT box binding proteins. Therefore, the competition between the activator of the CO complex and the repressors of TEMs for the respective binding sites leads to the precise control of the accumulation of *FT* to regulate flowering time (Castillejo and Pelaz, 2008). In addition, *TEM1* and *TEM2* also play pivotal roles in regulating flowering in the SAM by directly repressing *GA 3-oxidase 1 (GA3OX1)* and *GA3OX2* which encode enzymes catalyzing the last step of GA biosynthesis (Osnato et al., 2012). Therefore, the downregulation of *TEM1* and *TEM2* is needed to achieve enough expression of *FT* and *GA3OX1/2* to induce flowering. It seems that *TEM1* and

TEM2 have important roles both in leaves and SAM under LD and SD conditions (Osnato et al., 2012). Furthermore, *TEM1* and *TEM2* could interact with the N-terminal region of *GIGATEA* (GI), which regulates the expression of *CO* in a light-dependent manner in the vascular tissue, not only in vascular bundles but also in the mesophyll. This study suggested a model in which GI interacts with the repressors of *FT* including *TEM1/2* and *SVP* to transduce temperature and/or developmental signals by blocking their access to *FT* genomic regions and/or by affecting their stability and/or activity (Sawa and Kay, 2011).

1.5 *SEP4* functions in floral organ and meristem identity

MADS-box (for MINICHROMOSOME, AGAMOUS, DEFICIENS, and SERUM RESPONSE FACTOR) genes play fundamental roles in many eukaryotes. It has been hypothesized that an ancient duplication event occurring prior to the plant-animal divergence leads to the production of type I and type II MADS-box genes (Theissen et al., 1996). Type I genes includes the *ARG80/SRF*-like genes of animals and fungi and several similar genes in plants without the K-domain. Type II genes comprise the *MEF2*-like genes in animals and fungi and the MIKC-type genes in plants. MIKC-type proteins contain MADS-box (M), intervening (I), keratin-like (K) and C-terminal (C) domains. The MADS-box domain is found at the N-terminus and is the major determinant of DNA binding. MADS-box domain proteins bind to a consensus DNA site called the CArG box (CC (A/T)₆ GG). The I domain is relatively weakly conserved among plant MADS-domain proteins. In some *Arabidopsis* MADS-domain proteins, the I domain determines the selective formation of DNA-binding dimers (Riechmann et al., 1996). The K domain, which is only found in plant MADS-domain proteins so far, is involved in protein–

protein interaction primarily through hydrophobic residues and some charged residues. The C-terminal domain is the least conserved region in MIKC-type proteins. Some studies show that the C-terminal domain can enhance or stabilize the interactions mediated by the K-domain, and activates transcription in the presence of glutamine-rich or acidic stretches (Kaufmann et al., 2005).

SEPALLATA 4 (SEP4), which encoding a MIKC type MADS-box transcription factor, was first isolated as a floral organ identity gene. The “ABCE” model of floral organ identity is widely recognized. It describes how the A-, B-, C- and E-class genes specify the four whorls of floral organs (Coen and Meyerowitz, 1991; Litt and Kramer, 2010; Pelaz et al., 2001). *SEP4*, which belongs to the E-class genes, functions redundantly with other three homeotic genes, *SEP1*, *SEP2* and *SEP3*, in specifying floral organs (Ditta et al., 2004). All of the floral organ genes encode putative type-II MADS-box transcription regulators, except *AP2*. Unlike the other *SEP* genes that are expressed specifically in inflorescence tissues, *SEP4* is also expressed in the leaves and floral stems (Huang et al., 1995). Furthermore, *SEP4* protein has several potential sites for calmodulin-dependent phosphorylation and phosphorylation by casein kinase II, which implies more potential functions for *SEP4* (Huang et al., 1995).

Although *SEP* orthologs in other plant species are likely to play equally important roles in flower development, *SEP* genes play redundant and different roles in *Arabidopsis*. For example, in the *sep1 sep2 sep3* triple mutant, all the floral organs are converted into sepals, while in the *sep1 sep2 sep3 sep4* quadruple mutant, the floral organs are converted into leaf-like organs. These observations give us a hint that in addition to the roles in petal, stamen and carpel development, *SEP4* also plays an important role in sepal develop-

ment, which is relevant to A-class genes (Ditta et al., 2004).

SEP4 also plays a role in other developmental processes such as maintaining meristem identity. In *Arabidopsis*, the distinction between shoot and floral meristems is maintained by two antagonistic groups of genes. The first group of genes is the floral meristem identity genes, such as *LFY*, *API* and *CAL*, which are expressed in the floral meristems. Loss of their activity leads to various shoot-like characteristics. The representative gene in the second group is *TERMINAL FLOWER 1 (TFL1)* (Shannon and Meeks-Wagner, 1991), which prevents the shoot from becoming a flower and it is expressed in the centre of the shoot apex. A recent study has shown that *SEP4* play a redundant role with other three MADS-box genes in determining floral meristem identity through suppressing *TFL1* expression in the emerging floral meristems (Liu et al., 2013).

Expression analysis on *SEP4* has shown that this gene is widely expressed in many tissues, but our current knowledge regarding the function of *SEP4* is only limited to floral meristem and floral organ identity regulations. Given the broad expression spectrum of *SEP4*, it is not known whether *SEP4* also participates in regulating other developmental events in *Arabidopsis*. In this study, we present our preliminary findings showing that *SEP4* is also involved in the flowering time control.

1.6. Objectives of this study

The major objective of this project is to comprehensively elucidate *SEP4* function in flowering time control in *Arabidopsis* and its role in the flowering regulatory network. To achieve this goal, a series of genetic, molecular, biochemical and bioinformatic approaches have been and are being performed.

First of all, temporal and spatial expression patterns of *SEP4* have been examined to understand its potential role in flowering time control.

Secondly, *SEP4* expression in different flowering mutants and environmental conditions has been examined. In addition, we have investigated and are investigating *SEP4* expression in a variety of mutants that have flowering phenotypes, and the expression of other flowering time genes in *SEP4*-relevant mutants and transgenic plants. These studies will establish the genetic link between *SEP4* and other flowering time genes.

Thirdly, we are performing genetic crossing between *SEP4* genetic materials (*sep4* and *35S:SEP4*) and other mutants and transgenic plants in which the activities of other flowering time genes are altered. The genetic crossing results will substantiate the conclusion on *SEP4* genetic position in the flowering regulatory network.

Lastly, we have performed yeast-two hybrid screening to identify the interacting partners of *SEP4*, which gives us more cues on the molecular mechanism of how *SEP4* regulates flowering time. The relationship between *SEP4* and selected genes is being further confirmed by GST pull-down assay, co-immunoprecipitation (Co-IP), and bimolecular fluorescence complementation (BiFC).

CHAPTER 2:

MATERIALS AND METHODS

Chapter 2: Materials and methods

2.1 Plant materials and growth conditions

Wild-type and all mutants of *Arabidopsis thaliana* used in this study are in the Columbia (Col) background, except that *fve-1*, *fca-1* and *fpa-1* are in the Landsberg *erecta* (Ler) background. SALK line insertion mutants were purchased from the *Arabidopsis* Biological Resource Center (Ohio State University, USA). The 1.5kb p*TEM1-GUS* transgenic line was kindly provided by Prof. Soraya Pelaz, Centre for Research in Agricultural Genomics, Spain.

Arabidopsis were grown in long days (LDs) (16 h light/8 h dark) or short days (SDs) (8 h light/16 h dark) at 23 °C. Before the plants were transferred to the growth chamber, all seeds were sown and placed under 4°C for 3 days' stratification.

2.2 Genotyping

2.2.1 Extraction of genomic DNA

Plant leaf tissues were collected with a 1.5 ml Eppendorf tube and submerged in 200 µl of extraction buffer (0.2 M Tris-HCl pH 9.0, 25 mM EDTA, 1% SDS, and 0.4 M LiCl). After grinded by the plastic pestle, the suspension was centrifuged at maximal speed (14,000 rpm) for 8 min. The 120 µl supernatant was transferred to a new 1.5 ml Eppendorf tube and mixed well with the same volume of isopropanol. After centrifugation at maximal speed for 5 min, the supernatant was discarded and the pellet left in the tube was washed by adding 500 µl of 70% ethanol. The pellet was resuspended by vortexing and centrifuged for 5 min at maximal speed. Then the supernatant was discard-

ed again and the cell pellet was either air-dried by placing the tube upside down on a paper towel or dried by vacuum. In the end, the extracted genomic DNA was dissolved in 40 µl of either sterile water or TE buffer (10 mM Tris pH 8.0, 1 mM EDTA).

2.2.2 Genotyping Polymerase Chain Reaction (PCR) amplification

The genotyping PCR was performed with the specific primer sets listed in the Table 1. The PCR amplification systems were as follows: 0.5 µL DNA template (100 ng/µL), 2 µL 5 ×Green GoTaq® Reaction Buffer, 1 µL MgCl₂, 0.2 µL 10 mM dNTP mix, 0.3 µL upstream primer, 0.3 µL downstream primer, 0.05 µL GoTaq® DNA Polymerase and 5.75 µL nuclease-free water. The PCR products were analyzed by agarose gel electrophoresis.

Table 1. List of genotyping primers.

Mutant	Primers	Sequences
<i>sep4-1</i>	P1	5'-GCTTAGCATCTCTGCAAAACCAACACAAAGCTA-3'
	Bar-6x	5'-GATAGAGCGCCACAATAACAAACAATTGCGT-3'
	P2	5'-TGTACCTGCAAGTCTTTAGCTGATTGA-3'
<i>soc1-2</i>	P1	5'-TGTGTGCAAGGGAAATTAATAAAG-3'
	JMLB2	5'-TTGGGTGATGGTTCACGTAGTGGG-3'
	P2	5'-TGCCTCAGATAACGATCTATGGTAT-3'
<i>tem1-1</i>	P1	5'-AATCTCATGTGAACCCCCTTC-3'
	LBb1.3	5'-ATTTTGCCGATTCGGAAC-3'
	P2	5'-CGCTGATGCTTCTCGTAAATC-3'

2.3 Generation of transgenic plants

2.3.1 Construction of plasmid

The targeted DNA fragments were amplified with Phusion Hot Start II High-Fidelity DNA Polymerase (Thermo Scientific) using the mixing of cDNA or genomic DNA as templates. Then the products were purified with FavorPrep™ Gel/PCR Purification mini kit (Favorgen) either by PCR product purification or by gel extraction. Then the purified DNA fragments and the vectors were digested with the proper restriction enzymes and purified with the Gel/PCR Purification mini kit. The digested DNA fragments and vectors were mixed with ligation buffer and ligase then incubated at room temperature for 1 h or 16 °C overnight. Finally, the mixture was transformed into competent cells of *Escherichia coli* (*E.coli*) XL1-blue strain by heat shock transformation.

2.3.2 Heat shock transformation

The ligation mixture was added into the tube of *E.coli* competent cell and mixed gently by pipetting. After incubation on ice for 20 min, the tube was placed into a 42 °C water bath for 90 s then chilled on ice directly for 3 min. After that 1 mL LB medium was added into the tube and the culture was incubated at 37 °C shaker for 1 h. The culture was collected by centrifuged at 3,000 rpm for 3 min and the pellet was spread on LB agar plate supplemented with appropriate antibiotics. The plate was incubated at 37 °C for 16 h until the colony was suitable for colony PCR.

2.3.3 Colony PCR

Single colonies were picked up by white tips and resuspended in 6.5 µl sterile water

respectively. 1.5 µl of the cell suspension was used as template for PCR amplification with a gene specific primer and a vector specific primer. Then the PCR products were observed by agarose gel electrophoresis. The colonies which could be amplified to produce fragments with expected size were incubated in 3 ml LB medium with appropriate antibiotics at 37 °C overnight.

2.3.4 Plasmid extraction and DNA sequencing analysis

The plasmid DNA of the selected culture was extracted using FavorPrep™ Plasmid Extraction mini kit (Favorgen). The concentration of extracted plasmid DNA was analyzed by NanoDrop spectrophotometer (Thermoscientific. USA).

The plasmid DNA was sequenced by BigDye® Terminator v3.1 Cycle Sequencing Kit (Applied Biosystems). 100-300 ng of plasmid was mixed with 4 µl Big Dye, 2 pmol primer and topped up to 10 µl with sterile water. Sequencing PCR was programmed as follows: 25 cycles of denaturing at 96 °C for 10 sec, annealing at 52 °C for 5 sec and extension at 60 °C for 2 min. DNA sequencing was performed with ABI PRISM™ 377 DNA sequencer (Applied Biosystems, USA). And the sequences achieved were subsequently analyzed by BLAST tool on the Arabidopsis Information Resource (TAIR, www.arabidopsis.org) or the National Centre for Biotechnology Information (NCBI, www.ncbi.nlm.nih.gov).

2.3.5 Transformation into *Agrobacterium tumefaciens*

The transformation of the plasmid into *Agrobacterium tumefaciens* was performed by electroporation method. 100-200 ng plasmid was mixed gently with 40 µl thawed competent cell on ice. After incubation on ice for 30 min, the mixture was transferred into a pre-

chilled 1 mm Gene Pulser cuvette (Bio-Rad, USA) carefully avoiding any bubbles. Before the cuvette was placed into an electroporator, the outside of the cuvette should be wiped with tissues. The pulser was set as 25 μ F, 2.5 kV, 200 Ω and the pulse was 25 kV/cm. Then, the cell suspension was transferred to an Eppendorf tube with 1 ml LB medium and subsequently incubated at 28 °C for 3-6 h at a speed of 250 rpm. After incubation, cultured cells were collected by centrifugation for 10min at 3,000 rpm and the cell pellets were spread onto a LB agar plate supplemented with 50 mg/l tetracycline, 50 mg/l rifampicin and the appropriate antibiotics depending on the plasmid transformed. After incubation at 28 °C for 3 days, colonies were verified by colony PCR as section 2.3.3 described. Confirmed colonies were incubated in LB medium with the appropriate antibiotics at 28 °C shaker overnight.

2.3.6 Floral dip

The transformation of the target construct into *Arabidopsis* plants was performed by *Agrobacterium*-mediated floral dip method (Clough and Bent, 1998). The *Agrobacterium* was cultured in 50-100 ml LB liquid medium with the appropriate antibiotics at 28 °C for about 18 h until OD₆₀₀ reached 0.8-1.0. Cultured cells were harvested by centrifugation for 15 min at 4,000 rpm and re-suspended in 50 ml transformation medium (5% (w/v) sucrose with 0.015% (v/v) surfactant Silwet L-77). The floral buds of the plants were dipped into the bacteria suspension and submerged for 1 min. Then, the inoculated plants were covered to keep humidity and kept in dark condition for 16-24 h to improve transformation efficiency. After that, the plants were grown in the normal growth condition and the seeds were collected as T1 generation. In order to improve the yield, the dipping was repeated once after 2 weeks.

2.3.7 Selection of transgenic lines and genotyping

The T1 plants which were transformed with pGreen vectors and Gateway System vectors were selected by spraying 0.3 g/l Basta solution over 5-day-old seedlings. The survived T1 plants were confirmed whether the target construct was successfully integrated into the genome by genotyping PCR as previous described in section 2.2.2.

2.4 Expression analysis

2.4.1 Extraction of plant RNA

Total RNA was extracted using RNeasy® Plant Mini Kit (QIAGEN, USA) according to the user manual. Before use, all pipette tips, Eppendorf tubes and plastic pestles were autoclaved at 121 °C for 1 h to remove RNase. About 100 mg of plant tissues were frozen under liquid nitrogen and grounded thoroughly to a fine powder using a pestle in an Eppendorf tube. And the powder was suspended with 500 µl FARB Buffer (β-ME added) and vortexed vigorously. After incubated at room temperature for 5 min, the mixture was transferred into a filter column sitting in a 2 ml collection tube by pipetting. After centrifugation at full speed for 1 min, the clarified supernatant in the collection tube was carefully transferred to a new Eppendorf tube without disturbing the cell debris and pellet at the bottom. For each volume of the clear supernatant, 1 volume of 70% ethanol was added and mixed immediately by vortexing. The well mixed sample was then pipetted to a FARB mini column placed in a new 2 ml collection tube. After 1 min of centrifugation at full speed, the flow-through was discarded. To eliminate genomic DNA contamination, and 700 µl of Buffer RW1 was applied to the RNeasy® mini column, before washing the column by centrifugation of another 30 sec at maximal speed. The RNeasy® mini

column was then placed into a new 2 ml collection tube after discarding the collection tube with the flow-through. Subsequently, the RNeasy® mini column was added with 500 µl of Buffer RPE and then washed by centrifuging for 30 sec at top speed. The washing of the RNeasy® mini column with Buffer RPE was repeated once more, before the RNeasy® mini column was moved to a new 1.5 ml Eppendorf tube. 100 µl of RNase-free water was used for RNA elution by directly pipetting onto the silica-gel membrane of the RNeasy® mini column. Elution efficiency could be further increased by repeating the elution step with the first eluate. DNA contaminations could be removed from the total RNA samples, by incubating total RNA extracts on the RNeasy® mini column with RNase-free DNase (QIAGEN, USA) at 37 °C for 30 min between the two washing steps before the final elution. After that, the column was washed with wash buffer 1 once then wash buffer 2 twice. The column was dried with full speed centrifuge for 3 min. Finally, the RNA was eluted with 50 µL RNase-free water and measured by a NanoDrop spectrophotometer (Thermoscientific. USA).

2.4.2 Reverse transcription

The extracted RNA was reverse-transcribed into cDNA with the M-MLV Reverse Transcriptase according to the manufacture protocol (Promega, USA). 1 µg RNA was mixed with 2.5 µL 50 µM Oligo (dT)₂₀ then top up to 8.5 µL with RNase-free water. The mixture was denatured in the thermal cycler at 70 °C for 5 min then directly placed on ice. For each reaction, add 0.625 µl dNTP mix, 2.5 µl 5 × RT buffer, 0.31 µl Recombinant RNasin® Ribonuclease Inhibitor (40 U/µl) and 0.5 µl M-MLV RT (200 U/µl) and mix thoroughly by pipetting. The tubes were incubated at 37 °C for 1 h and 70 °C for 10 min. The cDNA products were diluted with 5 folds sterile water and could be directly used for

real-time PCR and semi-quantitatively RT-PCR or stored at -20 °C.

2.4.3 Quantitative real-time PCR

Real-time PCR was performed using the cDNA templates with SYBR Green PCR Master Mix (Thermo Scientific) on 7900HT Fast Real-Time PCR system (Applied Biosystems). Duplication or triplication reactions were needed with *TUBULIN2* (*TUB2*) as an internal control. The cycle threshold (Ct) difference between the target gene and *TUB2* ($\Delta C_t = C_{t(\text{target gene})} - C_{t_{TUB2}}$) was used to calculate the relative expression levels as $2^{-\Delta C_t}$. The specific primers used are listed in Table 2.

Table 2. List of quantitative real-time PCR primers.

Gene	Primers
<i>TUB2</i>	5'-GAGAATGCTGATGAGTGCATGG-3'
	5'-AGAGTTGAGTTGACCAGGGAACC-3'
<i>SEP4</i>	5'-GAGGATGGGAAGAGGGAAAG-3'
	5'-GAAGAGCAATCTCAGCATCA-3'
<i>FT</i>	5'-CTAGCCAGATGGAGAATAATCATCATG-3'
	5'-TTAAGGTGGCTAATTAAGTAGTAGTGGGAG-3'
<i>SVP</i>	5'-CAAGGACTTGACATTGAAGAGCTTCA-3'
	5'-CTGATCTCACTCATAATCTTGTCAC-3'
<i>TEM1</i>	5'-ACCAGACCGGCAATTGTATATCCAC-3'
	5'-ATCTCTTCTTGCCAACACACTCTACTG-3'
<i>TEM2</i>	5'-GACTAGAGCGGCAGTTATATAT-3'
	5'-CTTTCCACCGCAAACGGCCA-3'
<i>SMZ</i>	5'-AGGGAGAAGGAGCCATGAAGTTTGGTG-3'
	5'-GTCTTCAGAGGTTTCATGGTTGCCATG-3'
<i>SNZ</i>	5'-CAGCAGATTATTACATGGGTTTG-3'
	5'-GGTTTAATTTCTGTGATCGGTAGA-3'
<i>TOE1</i>	5'-CGAGTTATAATAATCCCGCCGA-3'
	5'-TTAAGGGTGTGGATAAAAGT-3'
<i>TOE2</i>	5'-ATGGAGAACCACATGGCTGC-3'
	5'-GGTGCTGTAGCTGCTACGGC-3'
<i>TOE3</i>	5'-ACGAGGAACGGTCATAATCTTG-3'
	5'-ATTCCCACCACTCGATTTCCT-3'

2.4.4 Semi-quantitative RT-PCR

Semi-quantitative RT-PCR of *sep4-1* was performed with specifically designed primers as listed in Table 3 and the length of product is about 500 bp. The expression level of *TUB2* was used as an internal control. The PCR products were analyzed by agarose gel electrophoresis.

Table 3. List of semi-quantitative RT-PCR primers.

Gene	Primers
<i>SEP4</i>	5' - GAGGACGGTTGATAAGTATAG-3'
	5' - GAAGAGCAATCTCAGCATCA-3'
<i>TUB2</i>	5' - ATCCGTGAAGAGTACCCAGAT-3'
	5' - TCACCTTCTTCATCCGCAGTT-3'

2.5 Gus staining

The GUS reporter transgenic lines were used to perform GUS staining following the methods described before (Sieburth and Meyerowitz, 1997). First of all, the tissues were fixed in the cold 90% acetone for 20-30 min followed by three times washing with the rinse solution (50 mM sodium phosphate pH 7.0, 1 mM potassium ferricyanide and 1 mM potassium ferrocyanide) on ice. Then the tissues were stained in the staining solution (the rinse solution with 2.0 mM X-Gluc) at 37 °C until the blue signals were visualized. After that, the tissues were washed with a series of ethanol to remove chlorophyll until the tissues were clear and kept in 100% ethanol. Eventually, the tissues were immersed in PBS solution or clearing solution (7.5 g gum Arabic, 100 g chloral hydrate, 5 ml glycerol and 30 ml water) and observed with light microscope. The primers designed for amplifying different promoter regions were listed in Table 4.

Table 4. List of promoter regions primers.

Promoter	Primers
2.6 kb <i>pSEP4</i>	5'- GGGCTGCAGGCATTTGCATATATCTCTATTG-3'
	5'- GGGGGATCCCAAGAAACCAAAACCCAAC-3'
1.5 kb <i>pTEM1</i>	5'-GGGTCGACGCCACGAAGAACTAAATCTGACCG-3'
	5'- GGGGATCCTTCTGACGTTGTACTACTGTCG-3'
3.1 kb <i>pTEM2</i>	5'- GGGAAGCTTAATTTACAAAAGTTTGATGTG-3'
	5'- GGGCTGCAGTTTCTTTGTTTCAGTTTCTTGAAG-3'

2.6 Yeast two-hybrid assay (small scale)

Yeast two-hybrid assay was performed following the Yeastmaker™ Yeast Transformation System 2 user manual (Clontech, USA). Genes of interest were cloned into pGADT7 (AD, GAL4 DNA activation domain) and pGBKT7 (BD, GAL4 DNA binding domain) vectors (Clontech, USA). Yeast strain AH109 was used in this yeast two-hybrid assay.

2.6.1 Preparation of competent yeast cells

Yeast strains stock was streaked on a YPDA agar plate [20 g/L difco peptone, 10 g/L yeast extract, 2% (w/v) glucose, 20 g/L Agar and 0.003% (w/v) adenine hemisulfate] and incubated at 30 °C for 3 days until the colonies appeared. A single colony was picked up and inoculated into 3 ml of YPDA liquid medium at 30 °C with shaking at 250 rpm for 8-12 h. 5 µl of the culture was transferred into 50 ml YPDA and incubated overnight until the OD600 reached 0.15-0.3. Then the cells were harvested by centrifugation at 700 × g for 5 min at room temperature and the pellets were resuspended in fresh 100ml YPDA to incubate for 3-5 h. When the OD600 reached 0.4-0.5, the cells were centrifuged at 700 × g for 5 min at room temperature and washed with 60 ml sterile deionized water. The harvested cells were subsequently resuspended in 3 ml 1.1 × TE/LiAc solution (diluted from 10 × LiAc (1 M LiAc pH 7.5) and 10 × TE (0.1 M Tris pH 7.5, 10 mM EDTA) with sterile water) and split into two 1.5 ml Eppendorf tubes. The tubes were centrifuged at top speed for 15 sec and the cells were resuspended in 600 µl 1.1 × TE/LiAc solutions as the competent cells ready for transformation.

2.6.2 Transformation of competent yeast cells

The AD and BD constructs containing the two genes of interest were cotransformed into the yeast competent cells. For each reaction, 5 μ l denatured Herring Testes Carrier DNA and 300 ng of each plasmid DNA were mixed in a sterile and prechilled 1.5 ml Eppendorf tube followed by adding 50 μ l prepared competent cells and mixing gently by vortexing. After adding 0.5 ml PEG/LiAc solution [50% (w/v) PEG 3350, 10 \times TE and 10 \times LiAc at the ratio of 8:1:1], the mixture was incubated at 30 $^{\circ}$ C for 30 min and mixed every 10 min. In the end of the PEG-mediated transformation, 20 μ l DMSO was added to terminate the reaction and the tube was placed in a 42 $^{\circ}$ C water bath for 15 min and mixed by vortexing every 5 min. The yeast cells were harvested by centrifuge at top speed for 15 sec and washed with 1ml 0.9% (w/v) NaCl solution. Finally, the cells were resuspended with about 50 μ l 0.9% (w/v) NaCl solution and separated onto SD/-Trp/-Leu, SD/-His/-Trp/-Leu and SD/-Ade/-His/-Trp/-Leu agar plates (Clontech, USA) equally. The plates were incubated at 30 $^{\circ}$ C for 3-6 days until colonies appeared.

2.7 Yeast two-hybrid screening using yeast mating

Yeast two-hybrid screening was performed with the MatchmakerTM Gold Yeast-Two Hybrid System (Clontech, USA) by yeast mating. In the Matchmaker GAL4-based two-hybrid assay, the bait protein, full-length SEP4 protein, was fused to the Gal4 DNA-binding domain (BD-SEP4), the libraries of prey proteins were fused to the Gal4 activation domain (AD). In this system, when the bait protein and prey protein interacted, the DNA-BD and AD would activate transcription of four independent reporter genes (*AURI-C*, *ADE2*, *HIS3*, and *MEL1*).

Firstly, *BD-SEP4* in pGBKT7 was transformed into Y2HGold strain (Clontech, USA) as the section 2.6 described. One fresh and large colony of the *BD-SEP4* strain was inoculated into 50 ml SD/-Trp liquid medium and incubated at 30 °C and 250-270 rpm for 16-20 h until the OD₆₀₀ reached 0.8. The cells were harvested by centrifugation at 1,000 g for 5 min and resuspended to a cell density of $> 1 \times 10^8$ cells per ml in 4-5 ml SD/-Trp liquid medium. Secondly, 1 ml aliquot of the library strain was thawed in a room temperature water bath and 10 µl of the strain was titered on 100 mm SD/-Leu agar plates for calculating the viability of the prey library. Then, the 4-5 ml bait strain was mixed with the library strain in a sterile 2 L flask with 45 ml 2 × YPDA liquid medium and 50 µg/ml kanamycin. The library vial was rinsed twice with 1ml 2 × YPDA and added to the flask. The flask was incubated at 30 °C for 20-24 h slowly shaking at a speed of 30-50 rpm. After 20 h incubation, a drop of the culture was checked under a phase contrast microscope (40 ×) to observe whether the 3-lobed zygotes were present. When the zygotes appeared, the cells were collected by centrifugation at 1,000 g for 10 min. and the flask was rinsed twice with 50 ml 0.5 × YPDA with 50 µg/ml kanamycin. The rinses were used to resuspend the pelleted cells and centrifuged to collect the cells at 1,000 g for 10 min. Thirdly, all of the pelleted cells were resuspended in 10 ml of 0.5 × YPDA with 50 µg/ml kanamycin and the total volume of cells and medium was measured. Then 100 µl of 1/10, 1/100, 1/1,000, and 1/10,000 dilutions of the mated culture were spread on each of the SD/-Trp, SD/-Leu and SD/-Leu/-Trp(DDO) agar plates and incubated at 30 °C for 3-5 days for calculating the number of clones screened [Number of Screened Clones=cfu/ml of diploids × resuspension volume (ml)]. The remain culture was spread on 50-55 150 mm DDO/X/A (SD/-Leu /-Trp/X-α-Gal/AbA) agar plates with 200 µl per plate and incu-

bated at 30 °C for 3-5 days. The mating efficiency ((No. of cfu/ml of diploids/ No. of cfu/ml of limiting partner) \times 100 = % Diploids) should be achieved between 2-5% to guarantee at least 1 million diploids were under screening. Finally, all the blue colonies growing on the DDO/X/A plates were patched out onto TDO/X/A plates with sterile pipette tips for more stringent selection.

All TDO/X/A positive interactions were picked up for further identification. Single colony was suspended in 5 μ l sterile water and frozen in liquid nitrogen then thawed at room temperature for three times to broken the yeast cells. 1.5 μ l of the cell suspension was used as template to perform PCR amplification with pGADT7 specific primers, pGAD-T7 (5'-TAATACGACTCACTATAGGG-3') and AD-R (5'-AGATGGTGCACGATGCACAG-3'). After agarose gel electrophoresis, each of the PCR products which showed a single and clear band was purification with FavorPrep™ Gel/PCR Purification mini kit (Favorgen). And the sequences of the fragments were analyzed by DNA sequencing and Blast to get their identities.

2.8 Chromatin Immunoprecipitation (ChIP) Assay

2.8.1 Nuclear fixation with formaldehyde

Fresh plant samples at proper stage were collected into 25 ml cold MC buffer (10 mM potassium phosphate pH7.0, 50 mM NaCl and 0.1 M sucrose). Then 37% formaldehyde stock was added into the MC buffer with a final concentration of 1%. The samples were fixed by applying vacuum for 40 min at 4 °C or on ice until the plant tissues became fully infiltrated and transparent. To terminate the fixation, glycine powder was added to a final concentration of 0.15 M and the samples were stirred at 4 °C for 20 min. Subsequently,

the samples were washed with new MC buffer by stirring at 4 °C for 20 min for three times and dried by clean tissue papers followed by frozen in the liquid nitrogen.

2.8.2 Nuclear protein-DNA extraction

The frozen samples were grinded with a mortar and pestle with liquid nitrogen until they became homogenous powder followed by adding 5 ml pre-cold M1 buffer (10 mM potassium phosphate pH 7.0, 0.1 M NaCl, 10 mM β -mercaptoethanol, 1 M hexylene glycol) with 1 mM PMSF. The slurry was filtered with a 0.45 μ m micro filter and transferred to a 2 ml Eppendorf tube. After centrifugation at top speed at 4 °C for 3 min, the pellet was washed with 2 ml pre-cold M2 buffer (10 mM potassium phosphate pH 7.0, 0.1 M NaCl, 10 mM β -mercaptoethanol, 1 M hexylene glycol, 10 mM MgCl₂, 0.5% Triton X-100) with freshly added protease inhibitor and centrifuged at top speed for 3 min for 3-4 times until the supernatant became light green. Subsequently, the pellet was washed twice with pre-cold M3 buffer (10 mM potassium phosphate pH 7.0, 0.1 M NaCl, 10 mM β -mercaptoethanol).

2.8.3 Sonication and immunoprecipitation

The nuclei pellet was resuspended in 0.5 ml pre-cold sonication buffer [10 mM potassium phosphate pH 7.0, 0.1 M NaCl, 10 mM EDTA pH 8.0, 0.5% (w/v) sarkosyl] and sonicated to produce genomic fragments around 300-500 bp. After centrifugation at top speed for 5 min at 4 °C, the supernatant was transferred into a new 1.5 ml Eppendorf tube and the pellet was resuspended with new 0.25 ml sonication buffer and centrifuged to collect the supernatant into the 1.5 ml tube. 75 μ l out of the total 750 μ l supernatant was saved at -20 °C and separated into 25 μ l for western blot and 50 μ l as the input sample.

The remaining chromatin solution was mixed with equal volumes of IP buffer [50 mM Hepes pH7.5, 150 mM KCl, 5 mM MgCl₂, 10 μ M ZnSO₄, 1% (v/v) Triton X-100, 0.05% (w/v) SDS], 30 μ l agarose beads, 0.3 μ l salmon sperm DNA and the specific antibody. The mixture was rotating at 4 $^{\circ}$ C for 2 h or overnight. After the incubation, the mixture was centrifuged at 2,500 rpm for 1 min and the beads were washed with 1 ml IP buffer by inverting on a rotator for 3 min twice. Subsequently, the beads were washed with high salt buffer (IP buffer with 350 mM NaCl), LNDET buffer (0.25 M LiCl, 1% Nonidet P-40, 1% (w/v) deoxycholate, 1mM EDTA) and TE buffer (10 mM Tris pH 7.5, 1 mM EDTA). The chromatin was eluted with 500 μ l elution buffer (50 mM Tris pH 8.0, 1% SDS and 10 mM EDTA) by incubating at 65 $^{\circ}$ C for 15 min followed by centrifugation at top speed for 2 min at room temperature. 25 μ l out of the 500 μ l eluted samples was for western blot as post-binding sample and the remaining was for DNA analysis. Western blot was used to detect whether the specific protein was pulled down by the antibody successfully.

2.8.4 DNA analysis

The protein and the chromatin fragments were reverse cross-linked by adding 5 M NaCl to a final concentration of 0.3 M and heating at 65 $^{\circ}$ C overnight. Then the mixture was incubated with 1 μ l RNase A at 37 $^{\circ}$ C for 30 min to degrade RNAs and incubated with 0.5 mg/ml Proteinase K at 45 $^{\circ}$ C for 1-2 h to degrade proteins. After that, the chromatin DNA fragments were purified with QIAquick PCR purification kit (QIAGEN, USA) and eluted with 50 μ l sterile water. 10 μ l out of the DNA with glycerol as loading dye was used to test the DNA size by agarose gel electrophoresis.

The enrichment of the DNA fragments was analyzed by real-time PCR and the input samples were diluted by 100 times as the input template. The specific primers were listed

in Table 5.

Table 5. List of ChIP assays primers.

Primer	Sequences
<i>TEM1 _1</i>	5'-TCCAAATCTCATGTGAACCC-3'
	5'-ATGGGCGATGTGTAATAGCA-3'
<i>TEM1 _2</i>	5'-CCAAACTAGGTAAGGACTTGTAGGAAA-3'
	5'-GGCTTTTCTTGAAACTATATTCGTCC-3'
<i>TEM2 _1</i>	5'-CGACCAACCTATCCAAAAGTC-3'
	5'-GCTCACATGAACCTATCCTCAC-3'
<i>TEM2 _2</i>	5'-CCTCCAAGCATCTAGAATGTCA-3'
	5'-TCGCATTGAAAAGAAACAATTT-3'
<i>TEM2 _3</i>	5'-AATGTTCTTACGCCGTTGAAA-3'
	5'-CGAGAAGGGCAGACAAAAAT-3'

2.9 Transient expression in tobacco plants

The transient expression of fluorescent fusion protein in tobacco (*Nicotiana benthamiana*) was performed following the paper published (Sparkes et al., 2006). To observe the subcellular location of SEP4, the CDS of *SEP4* was cloned into pGreen-35S:GFP vector to generate GFP-SEP4 fusion protein. The construct was transformed into the *Agrobacterium* as section 2.3.5 described. 3 ml of *Agrobacterium* culture was harvested by centrifugation at 3,000 rpm for 10 min and the pellet was resuspended with infiltration medium (10 mM MES, 10 mM MgCl₂, 100 μ M Aceto-syringone, pH 5.6) to a final OD₆₀₀ of 0.4-0.6. After being kept at room temperature for 2-3 h, the suspension was infiltrated into 3-4 weeks old tobacco leaves. The GFP signal was observed under microscope after two days. For Bimolecular Fluorescence Complementation (BiFC) assay, the CDSs of genes of interest were cloned into four pSAT1 vectors to create cYFP or nYFP-fusion proteins. The constructs were transformed into *Agrobacterium* and the cultures were co-infiltrated into tobacco leaves.

CHAPTER 3

RESULTS

Chapter 3: Results

3.1 Sequence analysis of *SEP4*

SEP4 contains an open reading frame of 774 bp and encodes a protein of 258 amino acids. The structure of *SEP4* is similar to the other three *SEP* proteins, *SEP1*, *SEP2* and *SEP3*. At the N-terminus, there is a highly conserved MADS-box domain. The K-domain located in the central region is less conserved. Like other MADS-box genes, the C-terminal region is highly different among the *SEP* proteins (Figure 2A). *SEP4* contains 4 potential phosphorylation (R/KXXS/T) sites (Figure 2B), implying that the activity of *SEP4* might be regulated by phosphorylation. In addition, *SEP4* contains glutamine-rich regions which are not found in other *SEP* proteins (Figure 2B). Glutamine-rich regions have been implicated as transcriptional activator, indicating that *SEP4* itself may directly serve as a transcriptional activator.

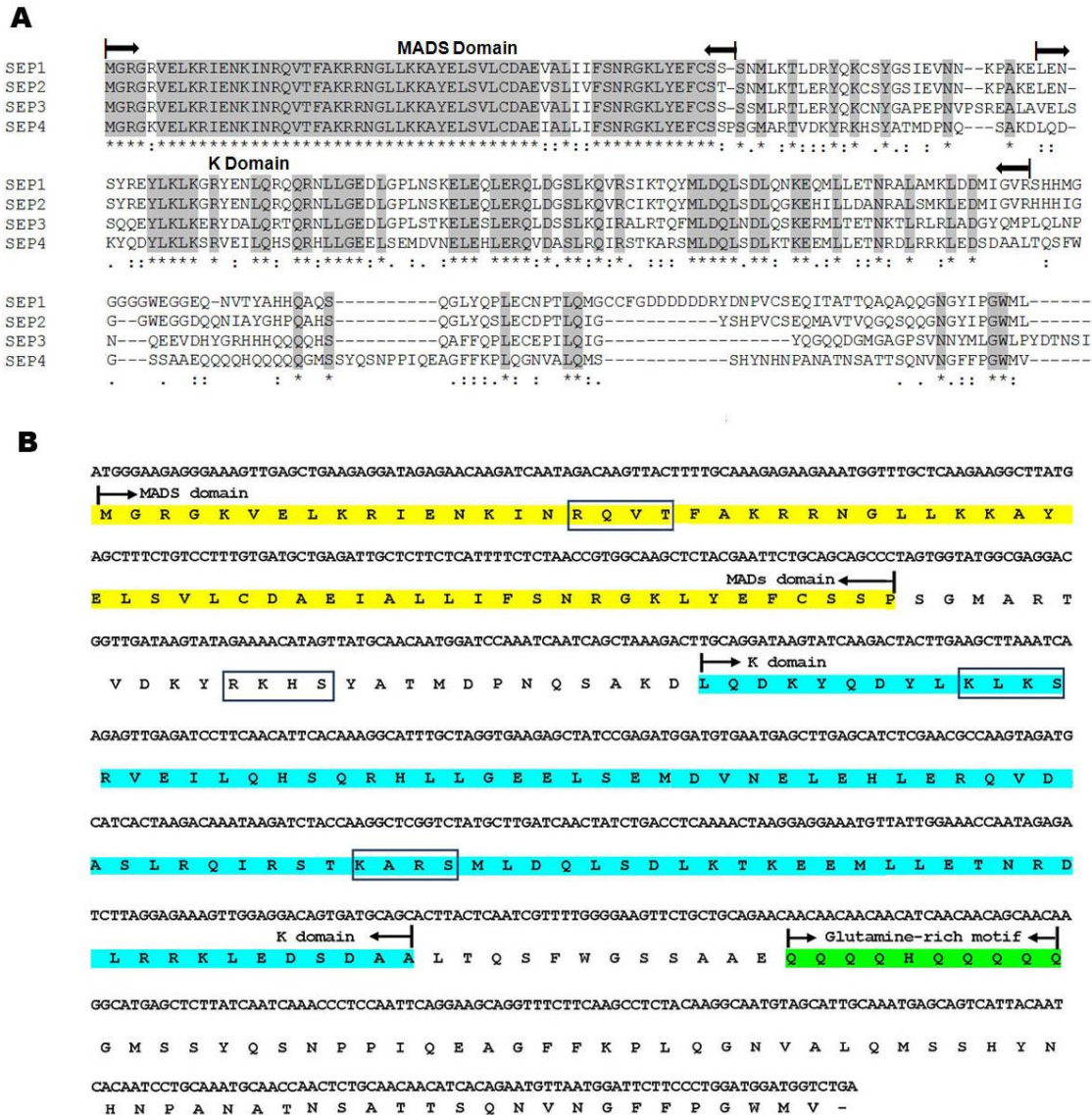


Figure 2. Bioinformatic analysis of *SEP4* sequence.

(A) Alignment of amino acid sequences of SEP family. Conserved residues are shown in grey.

(B) The *SEP4* CDS and amino acid sequences are shown. The MADS-box is highlighted in yellow and the K-box is in blue. The potential phosphorylation sites (R/KXXS/T) are highlighted in the boxes. The glutamine-rich stretch in the C-terminus is highlighted in green.

3.2 The *sep4-1* mutant shows indistinguishable phenotypes as wild-type, but overexpression of *SEP4* causes early flowering

In order to elucidate how *SEP4* functions in the reproductive development, we isolated a mutant (*sep4-1*) carrying a T-DNA insertion at the first intron (+307) from the University of Wisconsin Bio-technology Center (<http://www.biotech.wisc.edu/Arabidopsis/>) (Figure 3A). Semi-quantitative RT-PCR analysis revealed that there was no detectable expression of *SEP4* in *sep4-1* mutants, suggesting that *sep4-1* is a null mutant (Figure 3B). This single mutant showed a comparable flowering phenotype to wild-type plants (Figure 3B).

To further clarify whether *SEP4* plays a role in regulating flowering time, we generated 8 independent *SEP4* overexpression lines harboring the *SEP4* cDNA driven by the strong cauliflower mosaic virus (CaMV) 35S promoter (35S). Among these lines, 6 lines of the T1 generation flowered earlier than wild-type plants with an average of 7.3 rosette leaves under LD conditions (Figure 3C). Quantitative real-time PCR was applied to measure *SEP4* expression in a selected 35S: *SEP4* transgenic line and we found that *SEP4* expression was highly upregulated by about 30 times as compared to wild-type plants (Figure 3C). These observations indicate that *SEP4* could serve as a flowering activator.

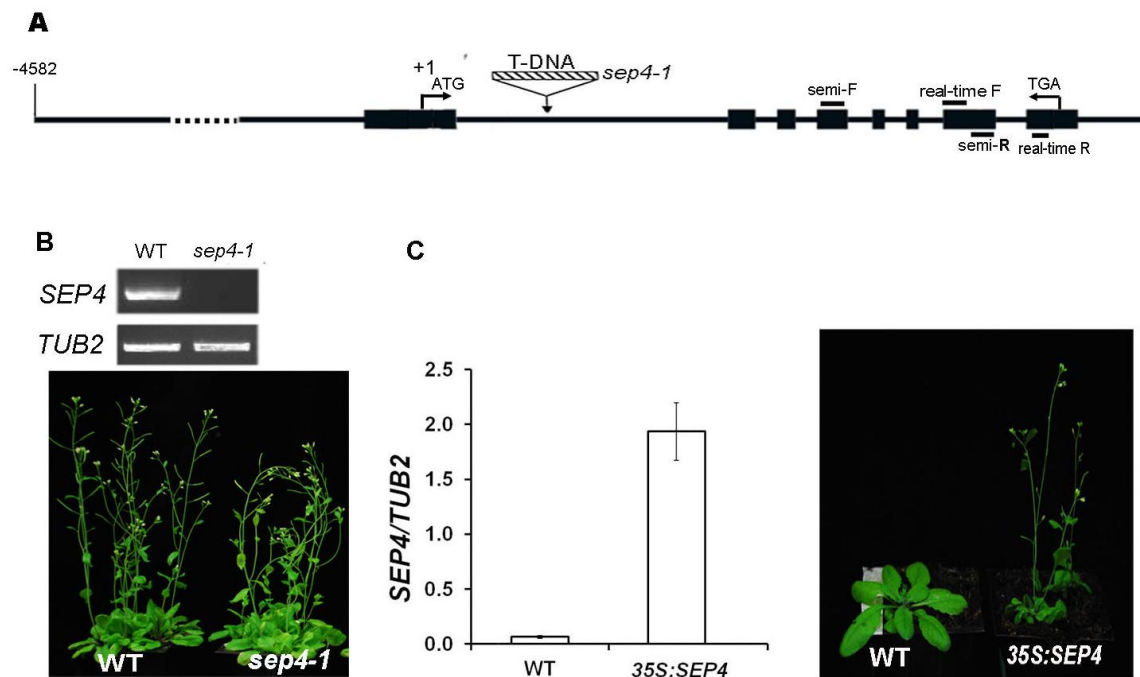


Figure 3. *SEP4* regulates flowering time in *Arabidopsis*.

(A) Schematic diagram of the *SEP4* genomic region. The exons are indicated by black boxes and the introns, the upstream and downstream regions are represented by black lines. The T-DNA insertion site is in the first intron. The primers for semi-quantitative RT-PCR and real-time PCR are shown.

(B) Semi-quantitative RT-PCR shows that *SEP4* expression is undetectable in *sep4-1*. *TUB2* was amplified as an internal control. Flowering phenotypes of *sep4-1* and WT grown in LDs are shown.

(C) Quantitative real-time PCR shows comparison of *SEP4* expression level (left panel) and flowering phenotypes (right panel) in WT and 35S:*SEP4*. Error bars denote SD.

3.3 Spatial and temporal expression patterns of *SEP4*

To analyze the spatial expression patterns of *SEP4*, quantitative real-time PCR was performed using total RNA extracted from various tissues of Col wild-type. *SEP4* transcripts were detected at different levels in almost all the plant tissues examined. The highest levels of transcripts were detected in cauline leaves followed by juvenile rosette leaves and stems (Figure 4A). In order to monitor the detailed expression patterns of *SEP4*, *pSEP4: GUS* reporter line was generated in which the GUS gene was driven by a 2.6-kb upstream genomic fragment from the *SEP4* start codon. Among 43 independent transgenic lines, 33 lines displayed similar expression patterns, and one representative line was chosen for the further detailed study. These results were consistent with the RNA blot results reported previously (Huang et al., 1995).

The temporal expression of *SEP4* was also examined by quantitative real-time PCR in developing seedlings. Under LD conditions, *SEP4* expression in wild-type plants was gradually upregulated from day 3 to day 9 after germination (Figure 5A). To further confirm the temporal expression pattern of *SEP4*, we performed GUS staining of *pSEP4: GUS* seedlings grown on MS medium in different days. The results displayed that the GUS signals detected in 5-, 7- and 9-day-old seedlings were stronger than that in 3-day-old seedlings (Figure 5B). Our results suggested that *SEP4* was expressed mainly in the leaves and stems, and the expression levels increased gradually over the developmental age, implying that *SEP4* might be involved in the control of flowering time.

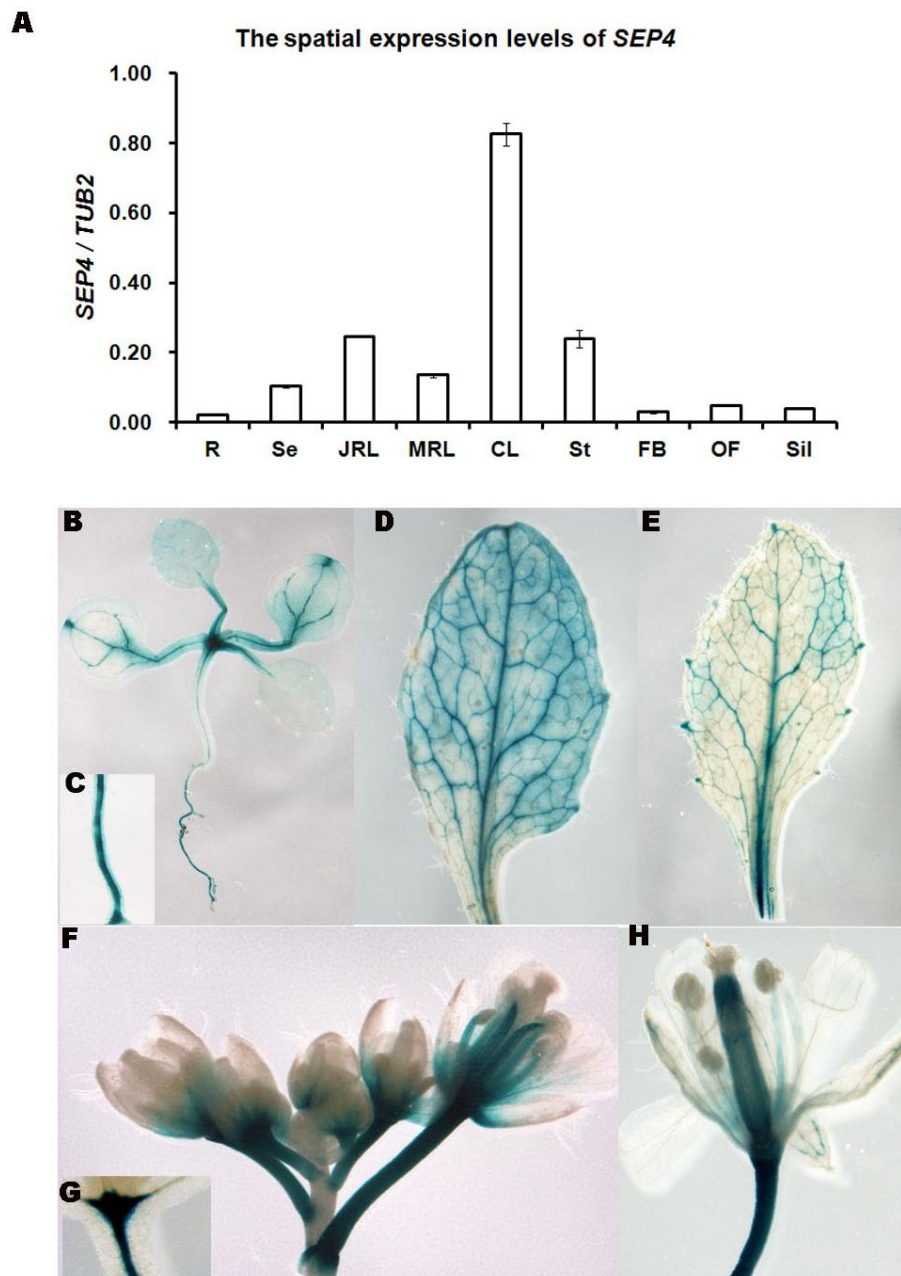


Figure 4. Spatial expression patterns of *SEP4*.

(A) Quantitative real-time PCR shows *SEP4* expression in different organs of wild-type plants. R, roots; Se, seedlings; JRL, juvenile rosette leaves; MRL, mature rosette leaves; CL, cauline leaves; St, inflorescence stems; FB, flower buds; OF, open flowers; Sil, siliques. *TUB2* was amplified as an internal control. Error bars denote SD

(B) to (H) Representative GUS staining of *pSEP4:GUS* transgenic plants shows a 5-day-old seedling (B), a primary root (C), a cauline leaf (D), a rosette leaf (E), inflorescence (F), shoot apical meristem (G), and an open flower (H).

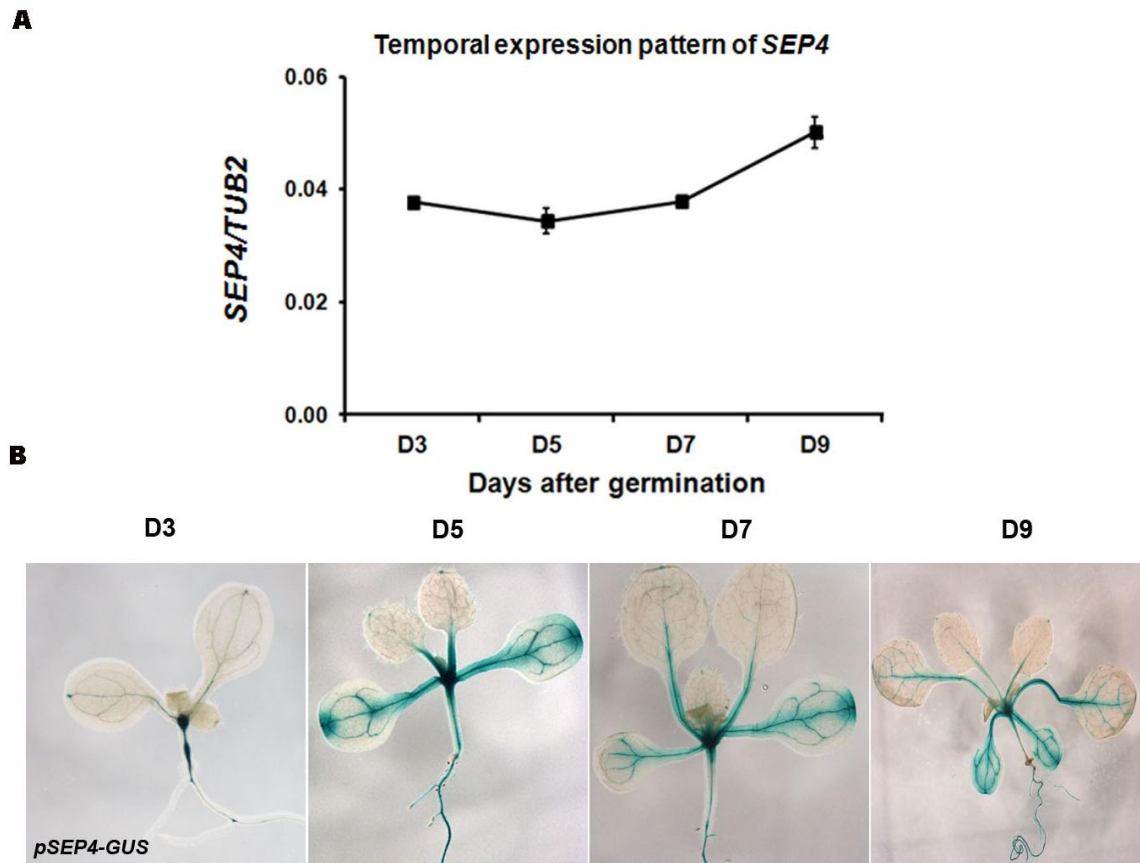


Figure 5. Temporal expression patterns of *SEP4*.

(A) Temporal expression pattern of *SEP4* determined by quantitative real-time PCR in wild-type plants grown under LDs. Error bars denote SD.

(B) GUS staining patterns of *pSEP4: GUS* transgenic lines grown on MS medium under LDs.

3.4 Subcellular localization of SEP4

As *SEP4* encodes a MADS-box transcription factor, we further investigate whether this protein is localized in the nucleus. To this end, we generated the *35S:GFP-SEP4* construct in which SEP4 protein sequence was fused to GFP, and the resulting construct was infiltrated into the tobacco leaves. GFP-SEP4 signals were detected in the nucleus (Figure 6), supporting its function as a transcription factor.

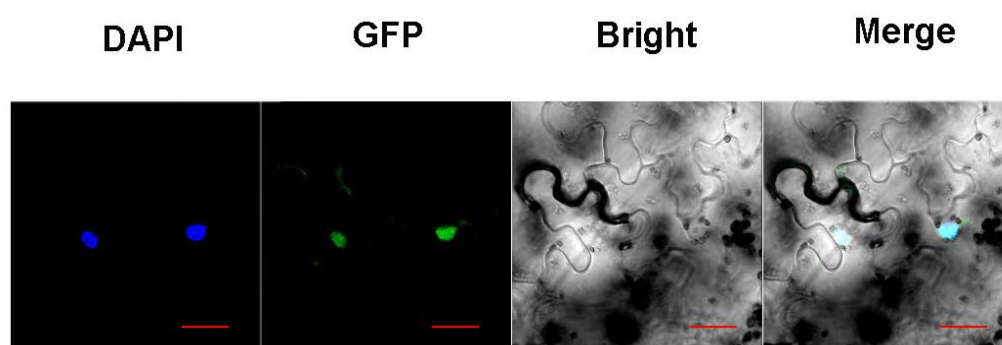


Figure 6. Subcellular localization of GFP-SEP4.

Subcellular localization of GFP-SEP4 in tobacco leaves infiltrated with *35S::GFP-SEP4*. DAPI, fluorescence of 4'6-diamidino-2-phenylindole. Bars = 20 μ m.

3.5 Investigation of flowering genetic pathways that regulate *SEP4* expression

In *Arabidopsis*, several flowering genetic pathways integrate the environmental and developmental inputs to regulate the delicate flowering process. To understand how *SEP4* regulates flowering in response to various flowering signals. *SEP4* expression was examined in different environmental conditions and in a variety of flowering mutants.

Firstly, we examined the expression of *SEP4* in different mutants in the autonomous and vernalization pathways. *SEP4* expression was downregulated in five autonomous pathway mutants including *fld-3*, *flk-3*, *fve-3*, *fve-1* and *fca-1* compared with wild-type (Figure 7A, B). However, *SEP4* expression in *flc-3* and *syp-41* mutants was comparable to that in wild-type plants (Figure 8A). These results suggest that *SEP4* expression is influenced by the autonomous pathway probably by a *FLC*- and *SVP*-independent way, which needs to be further investigated. While vernalization treatment didn't affect *SEP4* expression in both wild-type and *FRI/FLC* plants in which *FLC* expression was dramatically decreased (Figure 8B, C). The result was consistent with the findings that neither loss of *SEP4* nor overexpression of *SEP4* affects the sensitivity of plants in response to vernalization (Figure 8D). In conclusion, *SEP4* is not regulated by the vernalization pathway.

To test whether *SEP4* is affected by the GA pathway, wild-type plants were grown under SDs with or without 100 μ M GA treatment for 3 to 5 weeks and harvested for expression analysis. The quantitative real-time PCR results showed that the exogenous GA treatment didn't influence *SEP4* expression (Figure 9A). Furthermore, the expression of *SEP4* was not greatly changed in the GA-deficient mutant *gal-3* grown under SDs for 2 to 5 weeks as compared with wild-type plants (Figure 9B). In addition, the responses of

the *sep4-1* plants and *35S:SEP4* transgenic plants to the exogenous GA treatment were comparable to wild-type plants in flowering time control (Figure 9C). These results indicate that the GA pathway does not regulate *SEP4*.

In order to examine whether *SEP4* is regulated by the photoperiod pathway, we first examined *SEP4* expression in different photoperiod pathway mutants. The results showed that *SEP4* expression dramatically decreased in *co-1* and significantly decreased in *gi-1* mutants. There was no obvious change in *SEP4* expression in *ft-10* mutants (Figure 10A). To confirm the effect of these important photoperiod pathway genes, we also examined the expression of *SEP4* in 7-day-old and 9-day-old seedlings of *35S:CO* transgenic lines. *SEP4* was obviously upregulated in *CO* overexpression lines (Figure 10B). These results indicate that *SEP4* is regulated by the photoperiod pathway and functions as a downstream target of *CO*. Because *CO* mediates the effect of circadian clock on flowering in *Arabidopsis*, we further examined *SEP4* expression levels every 2 hours within a day under LDs. The quantitative real-time PCR results demonstrated that *SEP4* expression was increased in the dark and peaked at dawn when *FT* expression reached to the peak during 24 hours (Figure 10C, D).

Taken together, our results suggest that the autonomous and photoperiod pathways, but not the vernalization pathway and GA pathway, regulate *SEP4* expression.

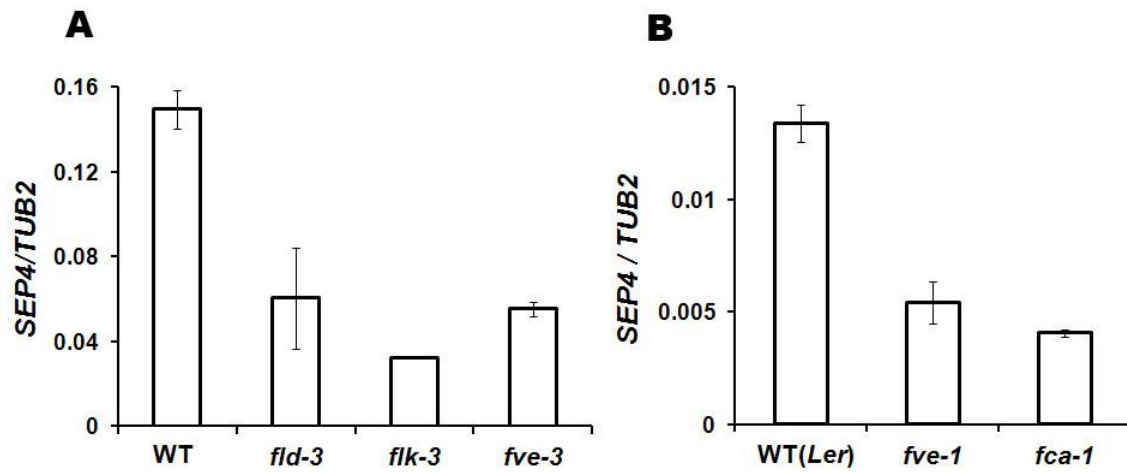


Figure 7. *SEP4* expression is affected by the autonomous pathway.

SEP4 expression in different autonomous pathway mutants under Col background (A) and *Ler* background (B) was determined by quantitative real-time PCR. 9-day-old seedlings grown under LDs were harvested for expression analysis. Error bars denote SD.

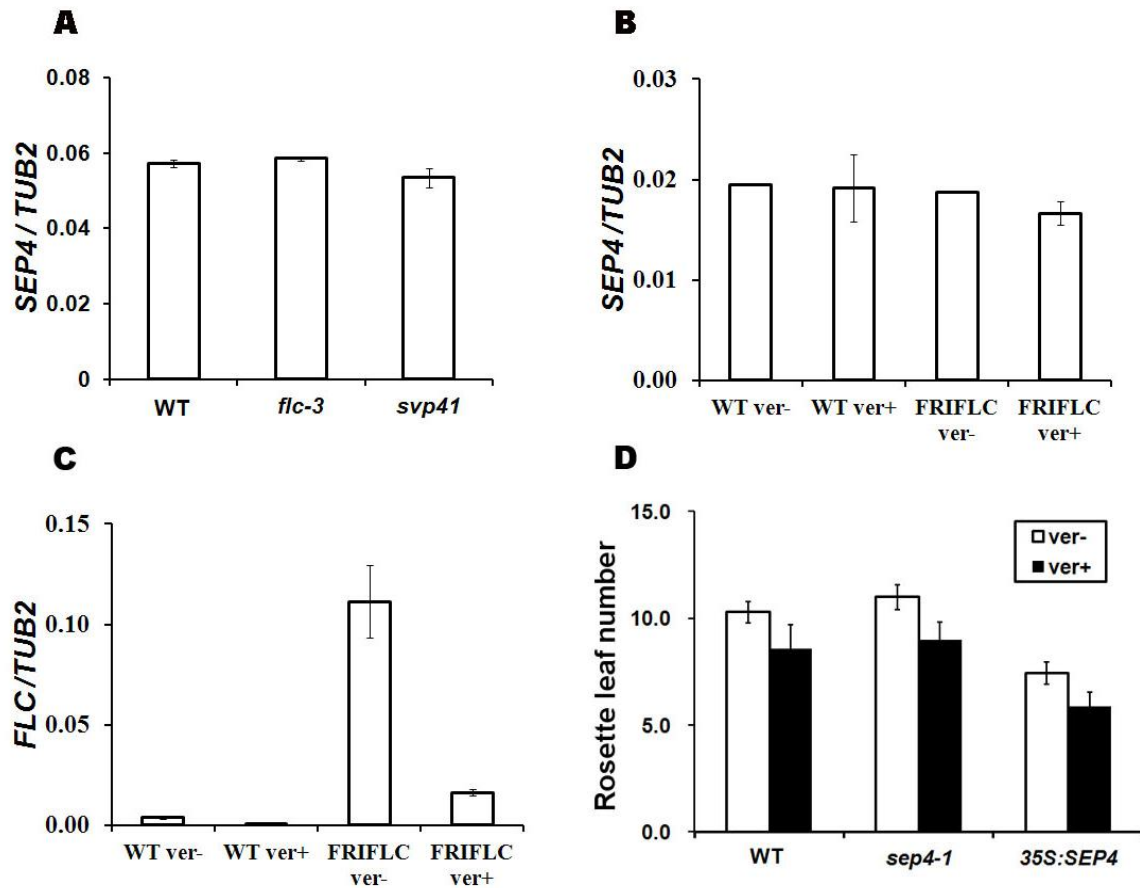


Figure 8. *SEP4* expression is not affected by the vernalization pathway.

(A) *SEP4* expression in 9-days-old *flc-3* and *svp41* mutants determined by quantitative real-time PCR. Error bars denote SD.

(B and C) Expression levels of *SEP4* and *FLC* with and without vernalization treatment determined by quantitative real-time PCR. Seeds were grown on MS medium and vernalized at 4 °C under low light condition for 8 weeks. 9-day-old seedlings grown under LDs were harvested for expression analysis. Error bars denote SD.

(D) Flowering time of wild-type, *sep4-1* and *35S:SEP4* with or without vernalization treatment. Error bars denote SD.

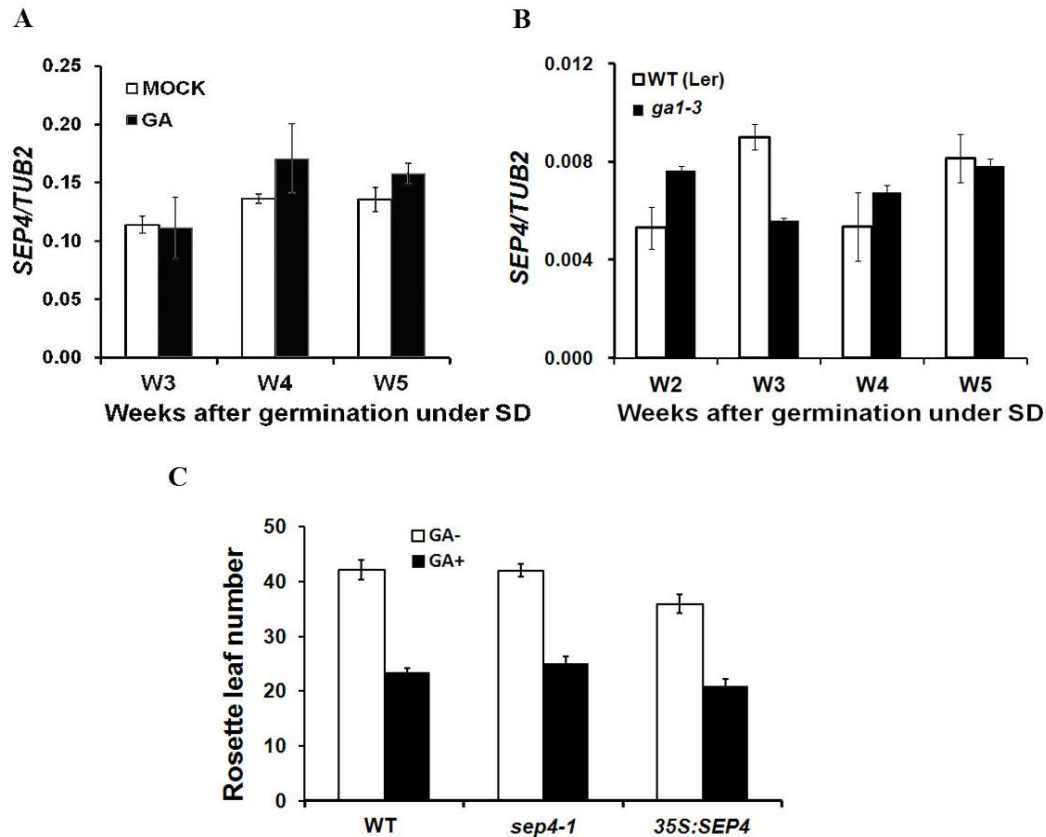


Figure 9. *SEP4* expression is not affected by the GA pathway.

(A) Effects of GA treatment on *SEP4* expression determined by quantitative real-time PCR. Wild-type plants (Col background) were treated weekly with exogenous GA (100 μ M). Seedlings treated for 3 (W3), 4 (W4) and 5 (W5) weeks were harvested for expression analysis. Error bars denote SD.

(B) *SEP4* expression determined by quantitative real-time PCR in the GA-deficient mutant *gal-3* (Ler background) and Ler wild-type plants. 2-, 3-, 4- and 5-week-old seedlings grown under SDs were harvested for expression analysis. Error bars denote SD.

(C) Flowering time of wild-type, *sep4-1* and *35S:SEP4* plants with 100 μ M GA or mock (0.1% ethanol) treatment twice a week under SDs from 3 weeks after germination. Error bars denote SD.

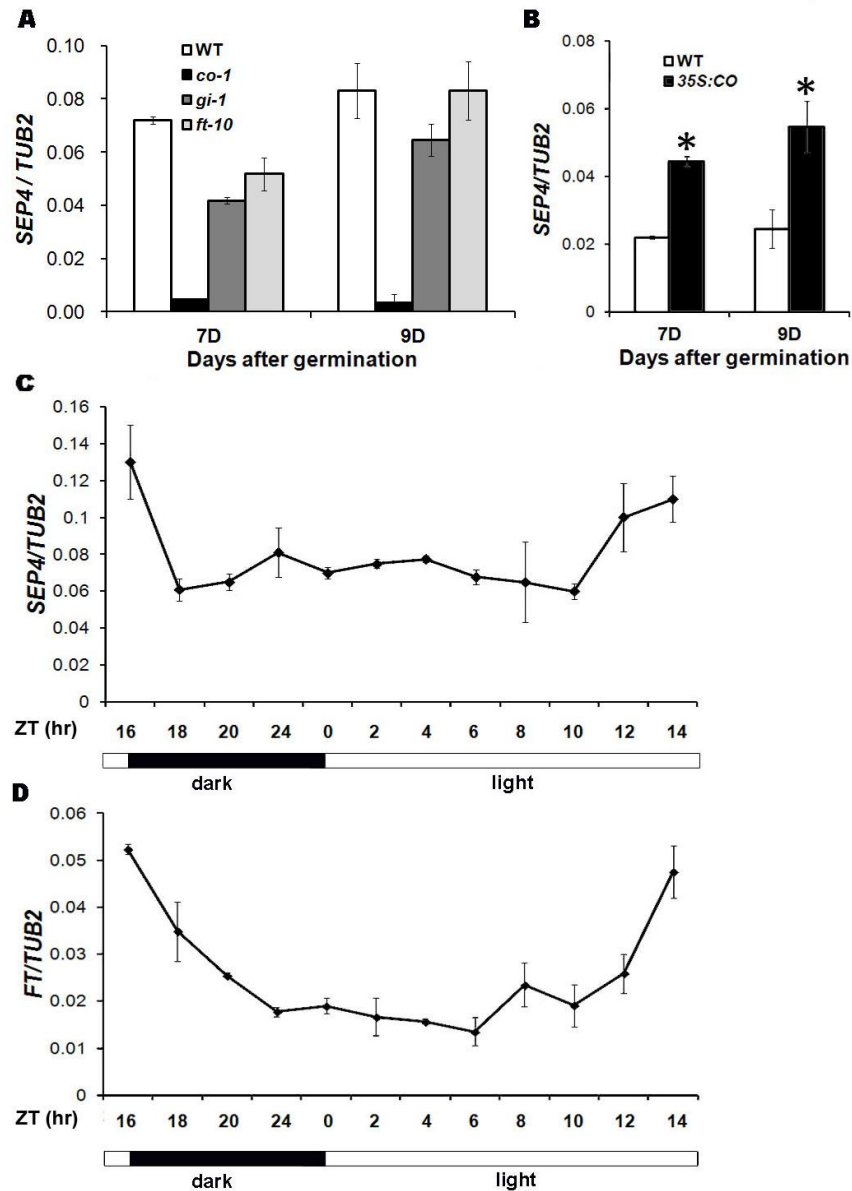


Figure 10. *SEP4* expression is affected by the photoperiod pathway.

(A) *SEP4* expression in photoperiod pathway mutants under LDs. Error bars denote SD.

(B) *SEP4* expression in transgenic plants overexpressing *CO*. Error bars denote SD. Asterisks indicate significant difference in the expression levels in the mutants as compared to that of wild-type plants (Student's test, $P < 0.05$).

(C and D) Diurnal oscillation of *SEP4* and *FT* mRNA abundance under long days (LDs). Black bars represent dark and white bars represent light. *FT* expression was detected as a positive control of the circadian clock. Error bars denote SD.

3.6 *sep4-1* single mutant enhances the late flowering phenotype of *soc1-2*

We also analyzed the genetic interactions between *SEP4* and other flowering time genes that function downstream of multiple flowering pathways. A comparison of flowering time among *sep4-1*, *35S:SEP4* and other flowering mutants showed that *sep4-1* could significantly enhance the late-flowering phenotype of *soc1-2* (Figure 11A-C), implying that *SEP4* has a redundant function with *SOC1* in promoting flowering. Because *sep4-1* single mutant didn't show significant flowering time phenotype, we performed comparative study between *soc1-2 sep4-1* and *soc1-2* in subsequently studies to reveal the downstream targets of *SEP4*.

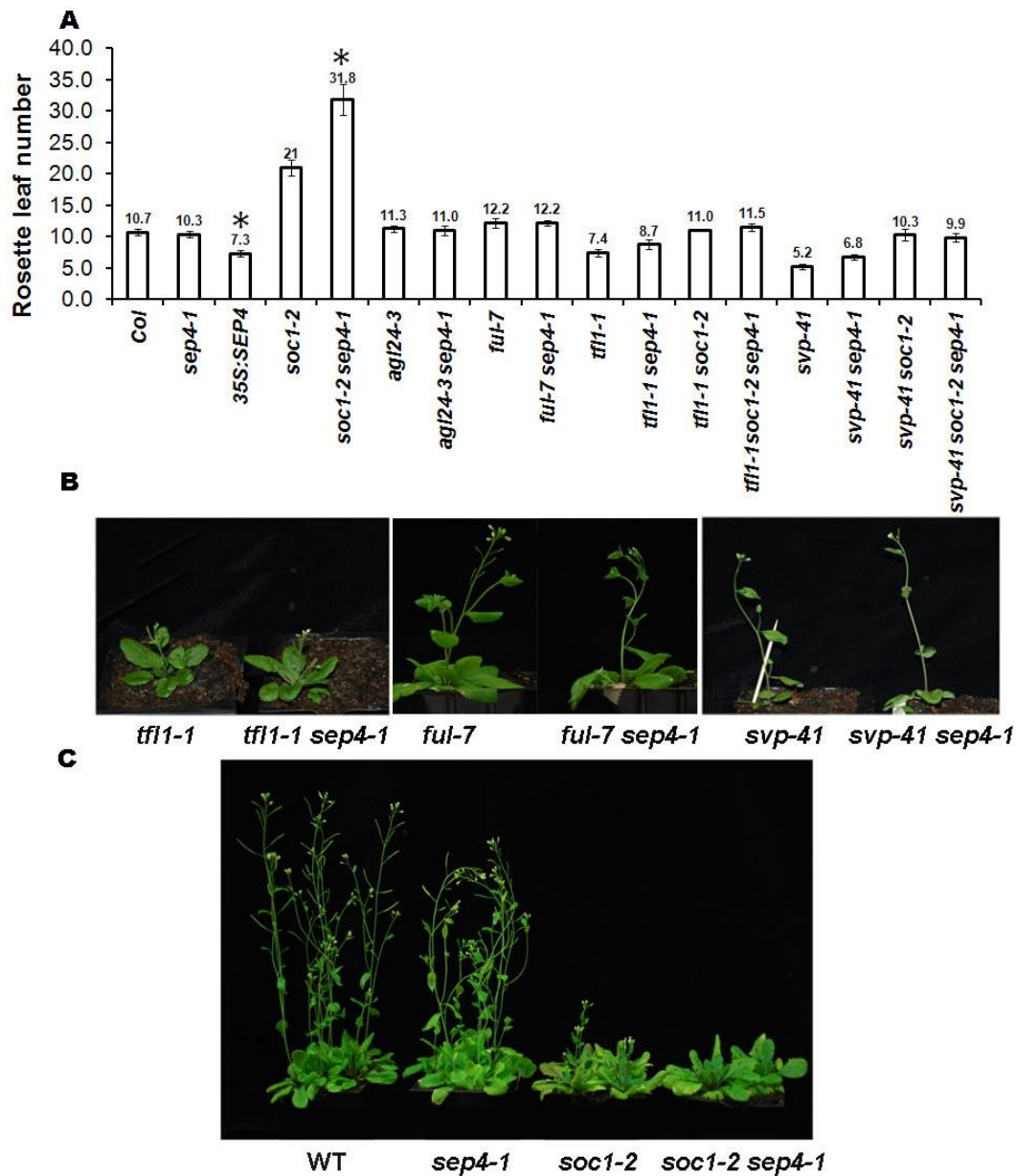


Figure 11. Loss of function of *SEP4* enhances the late-flowering phenotype of *soc1-2*.

(A) Flowering time of various mutants and transgenic plants grown under LDs. Values were scored from at least 15 plants of each genotype. The mean values of rosette leaf numbers are indicated on top of bars. Error bars denote SD. Asterisks indicate significant difference in flowering time of plants under various genetic backgrounds as compared with that of wild-type or *soc1-2*.

(B and C) Flowering phenotypes of various combination of *sep4-1* with other flowering time mutants.

3.7 Identification of *SEP4* downstream genes

Since *SEP4* has been found to be involved in the autonomous and photoperiod pathways, we examined whether it affects the key genes that are affected by these two pathways. First, we examined the expression levels of two potent transcriptional repressors, *FLC* and *SVP*, downstream of the autonomous pathway, in 9-day-old seedlings of *35S:SEP4*. Quantitative real-time PCR results showed comparable expression levels of *FLC* and *SVP* in *SEP4* overexpression lines with that in wild-type plants (Figure 12A) , The same results were obtained in *soc1-2 sep4-1* mutants (data not shown). These results suggest that *SVP* and *FLC* do not act downstream of *SEP4*.

On the contrary, the expression of *FT* in *soc1-2 sep4-1* double mutants was obviously downregulated compared to *soc1-2* and wild-type plants in the developing seedlings (Figure 12B), suggesting that *FT* expression is promoted by *SEP4*. Further, the GUS activities of *FT: GUS* under wild-type, *sep4-1*, *soc1-2* and *soc1-2 sep4-1* backgrounds were monitored. The results showed that *FT:GUS* signals were significantly reduced in the vasculature tissues in *soc1-2 sep4-1* double mutants compared with that in wild-type, *sep4-1* and *soc1-2* plants (Figure 12C). These results suggested that *FT* is the downstream gene of *SEP4* in flowering time control.

As *soc1-2 sep4-1* mutants showed enhanced late-flowering phenotype as compared with *soc1-2*, we also tested the effects of *SEP4* on the genes that are downstream of *SOC1* and upstream of *FT*, including *TEM1*, *TEM2*, *TOE1*, *TOE2*, *TOE3*, *SMZ* and *SNZ*. The quantitative real-time PCR results show that among these repressors of *FT*, *TEM1* and *TEM2* expressions were significantly upregulated in *soc1-2 sep4-1* mutants (Figure 13 A and B), demonstrating that the downregulation of *FT* in *soc1-2 sep4-1* might be me-

diated by derepressing the upstream repressors of *FT*. While the expressions of other five regulators were not affected (Figure 13C).

Next, we used *TEM1* and *TEM2* reporter lines to further study the spatial and temporal regulations of these genes by *SEP4*. The *pTEM1:GUS* reporter line, which was kindly provided by Prof. Soraya Pelaz (Castillejo and Pelaz, 2008), contains the 1.5 kb promoter sequence. While the *pTEM2* GUS reporter line generated by us contains the 3.1 kb genomic fragment from *TEM2* locus. The tissue expression patterns of *TEM1* and *TEM2* were first analyzed by quantitative real-time PCR. Both of them were highly expressed in the juvenile rosette leaves (Figure 14A, 15A). Furthermore, we examined the GUS staining patterns of the established *pTEM1: GUS* lines under *soc1-2* and *soc1-2 sep4-1* background. In agreement with the expression results (Figure 13A), the clear *TEM1* signal in the true leaves was much stronger in *soc1-2 sep4-1* compared with that in *soc1-2* and wild-type (Figure 14 B). The similar work with *pTEM2* GUS reporter line is still in progress.

As previously reported, SOC1 could specifically bind to the CArG box, which is 819 bp away from the start codon in the 5' promoter region of *TEM1*, with 3-fold enrichment in wild-type against in *soc1-2* single mutants, while the binding enrichment of SOC1 in the promoter region of *TEM2* was about 1.5 folds (Tao et al., 2012). To investigate whether SEP4 could directly bind to the putative targets when SOC1 was missing, a Chromatin Immunoprecipitation (ChIP) assay was performed with 9-day-old *soc1-2* mutants and wild-type plants. The antibody was tested by western blot and it could successfully bind to SEP4 proteins (Figure 16A). And after sonication the sizes of chromatin fragments were between 200 bp to 500 bp (Figure 16B). We used the same primers as Tao

used in her papers, which covered all the CArG boxes in *TEM1* and *TEM2* genomic regions (Figure 16D) (Tao et al., 2012). The results showed a 2.87-fold enrichment in the same promoter region of *TEM1* in *soc1-2* mutants compared with wild-type. And there were about 1.79-fold enrichment in the TEM2_1 region and 2.27-fold enrichment in the TEM2_3 region (Figure 16C). The results suggested that SEP4 could bind to the same binding sites as SOC1 in the promoter regions of *TEM1* and *TEM2*.

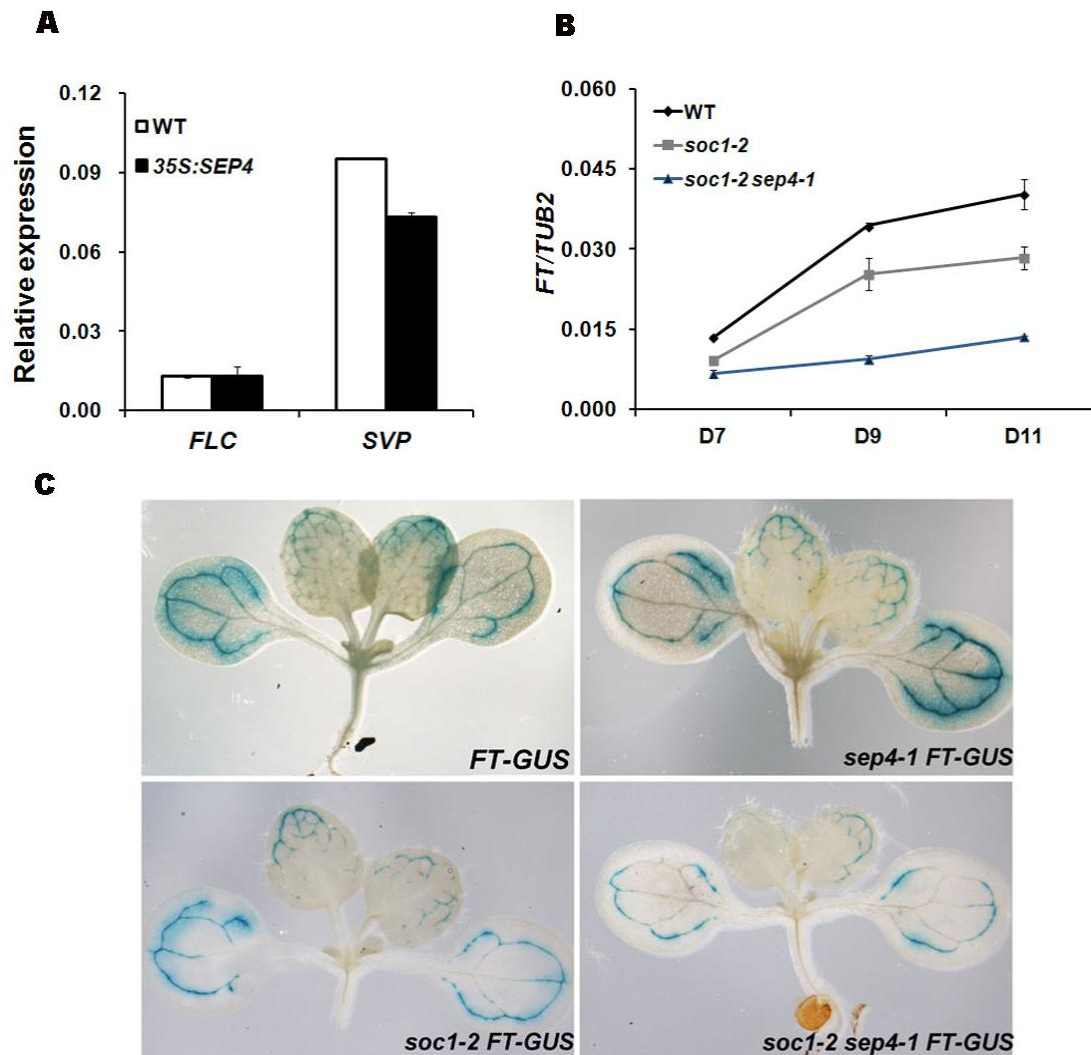


Figure 12. *FT* expression is regulated by *SEP4*.

(A) *FLC* and *SVP* expression in 9-day-old *35S:SEP4* and wild-type plants under LDs. Error bars denote SD. The expression was normalized with *TUB2* acting as an internal control.

(B) Temporal *FT* expression determined by quantitative real-time PCR in 7, 9 and 11-day-old *soc1-2*, *soc1-2 sep4-1* and wild-type plants under LDs. Error bars denote SD.

(C) GUS staining of *FT: GUS* under 7-day-old wild-type, *sep4-1*, *soc1-2* and *soc1-2 sep4-1* backgrounds.

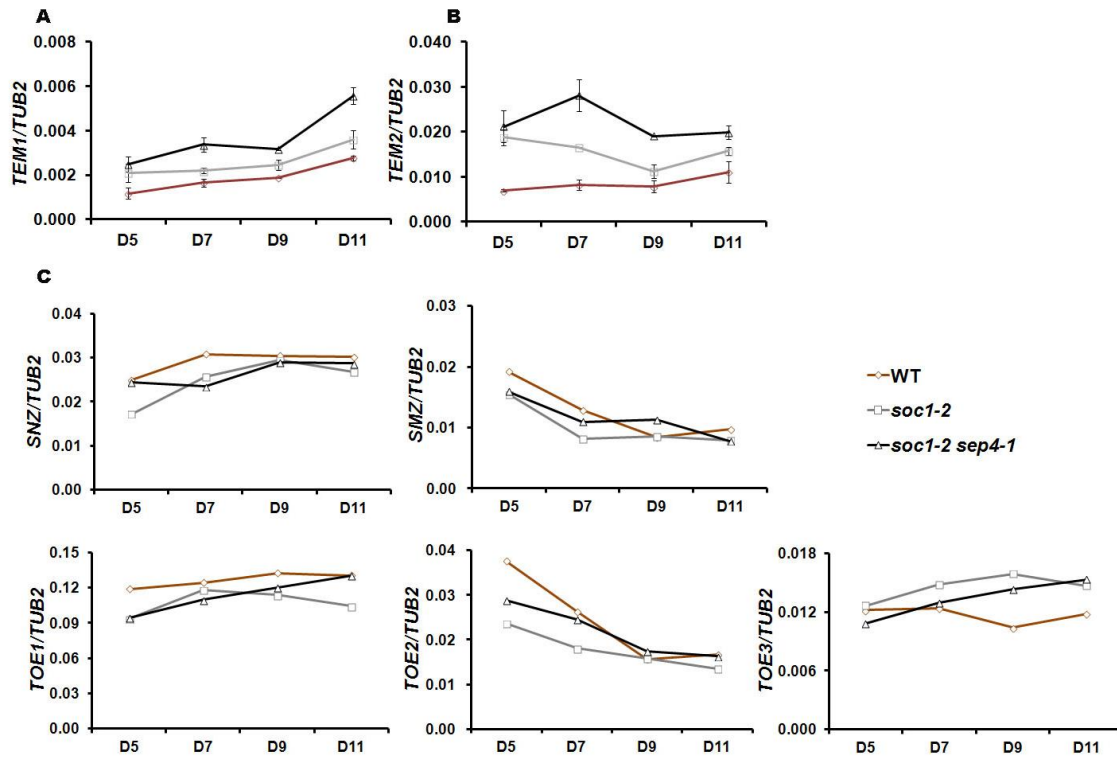


Figure 13. *TEM1* and *TEM2* expressions are upregulated in *soc1-2 sep4-1* plants.

Temporal expression of *TEM1*, *TEM2*, *SNZ*, *SMZ*, *TOE1*, *TOE2* and *TOE3* were determined by quantitative real-time PCR in developing seedlings of wild-type, *soc1-2* and *soc1-2 sep4-1* under LDs. Error bars denotes SD.

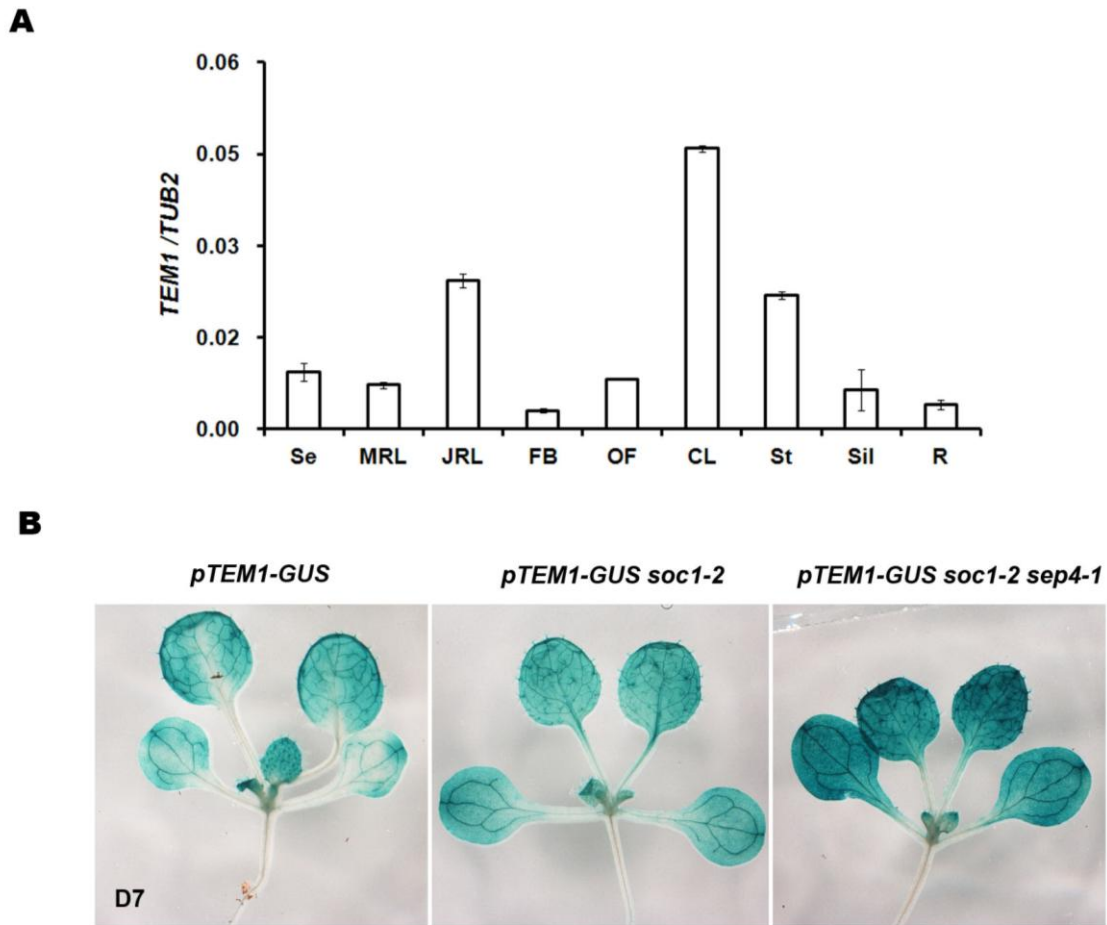


Figure 14. *TEM1* expression is regulated by *SEP4*.

(A) Spatial expression pattern of *TEM1* determined by quantitative real-time PCR in wild-type plants grown under LDs. Error bars denote SD.

(B) GUS staining of *pTEM1: GUS* in 7-day-old seedlings under wild-type, *soc1-2* and *soc1-2 sep4-1* backgrounds.

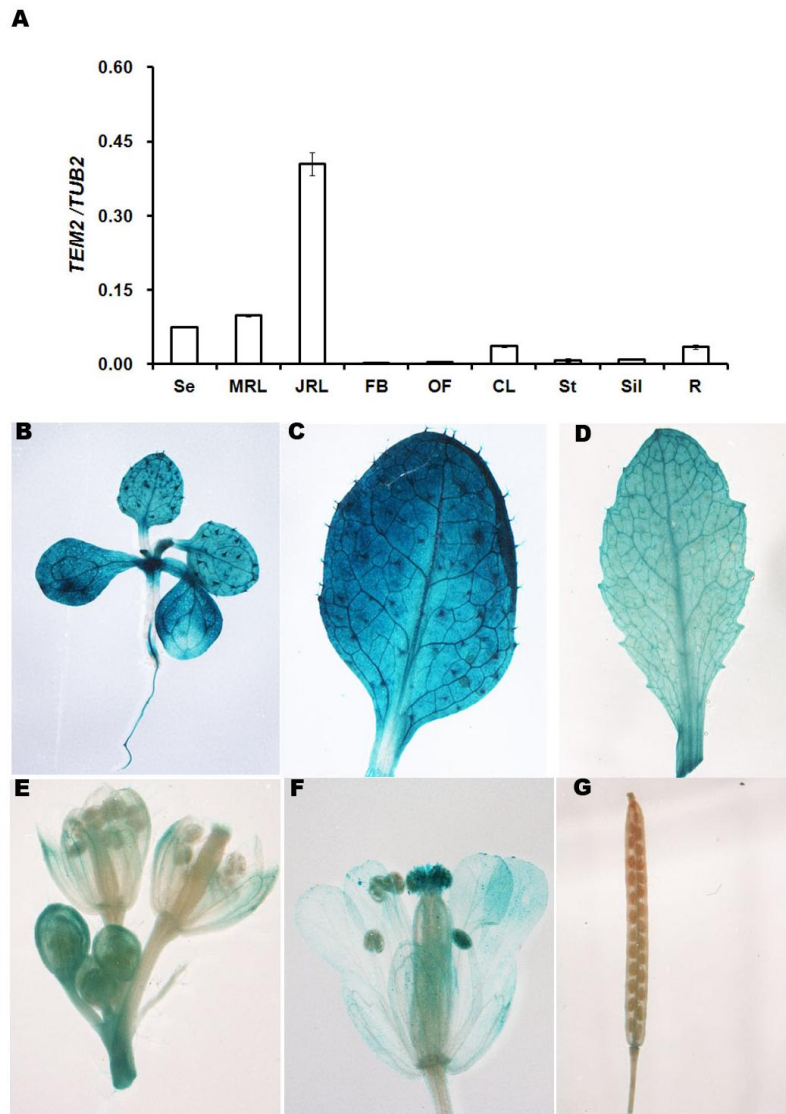


Figure 15. Spatial expression patterns of *TEM2*.

(A) Quantitative real-time PCR shows *TEM2* expression in different organs of wild-type plants. Se, seedlings; MRL, mature rosette leaves; JRL, juvenile rosette leaves; FB, flower buds; OF, open flowers; CL, cauline leaves; St, inflorescence stems; Sil, siliques; R, roots. *TUB2* was amplified as an internal control.

(B) to (G) Representative GUS staining of *pTEM2:GUS* transgenic plants shows a 5-day-old seedling (B), a mature rosette leaf (C), a cauline leaf (D), inflorescence (E), an open flower (F) and a silique (G).

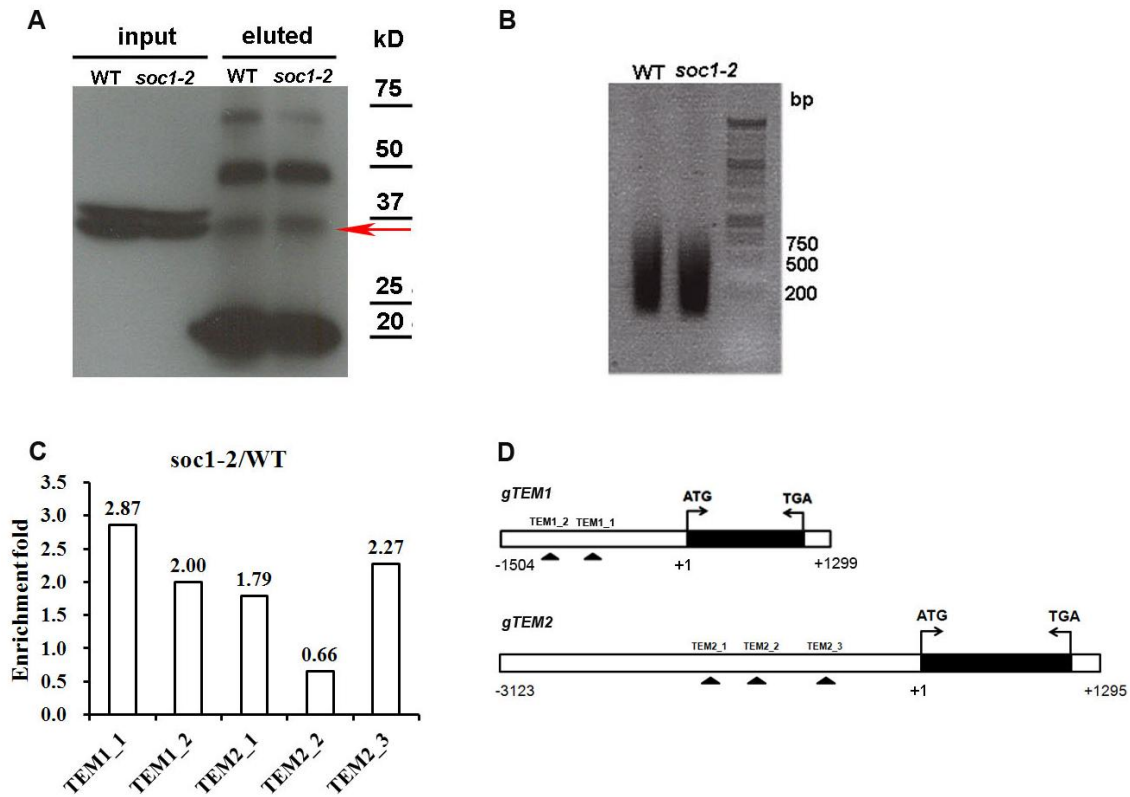


Figure 16. *SEP4* is directly associated with *TEM1* and *TEM2* chromatin.

(A) Western blotting shows the binding of *SEP4* antibody. The red arrow displays the size of *SEP4* protein.

(B) Agarose gel electrophoresis shows the chromatin fragments after sonication.

(C) ChIP enrichment test shows binding of *SEP4* to *TEM1* and *TEM2* genomic regions. Enrichment folds were calculated first by normalizing the amount of a target DNA fragment against genomic fragment of *TUB2*, and then by normalizing the value for *soc1-2* against that for wild-type.

(D) Schematic diagram shows the *TEM1* and *TEM2* genomic regions. Exons are represented by black boxes, while upstream and 3'UTR regions are represented by white boxes. Bent arrows denote translational start site and stop codon.

3.8 SOC1 and FUL are interaction partners of SEP4

As a MADS-box protein, SEP4 is supposed to play its roles as homo- or heterodimers with other MADS-box proteins as it regulates floral organ development and flower meristem identity. Therefore, we examined the interaction between SEP4 and other MADS-box proteins such as SOC1, AGL24, SVP, and FLC, which are involved in flowering time control. In addition, FUL was also chosen because the *ful-2* mutant enhances the late flowering phenotype of *soc1-2* (Melzer et al., 2008). Our yeast-two hybridization results showed that SEP4 could strongly interact with itself, SOC1 and FUL (Figure 17A and B). These interactions were confirmed by Bimolecular Fluorescence Complementation (BiFC) experiment, which monitors the protein-protein interaction through detecting the fluorescence signals emitted by the reconstitution of an enhanced yellow fluorescent protein (EYFP) from two fragments (N- and C- terminal halves) fused to two interacting proteins, respectively. The interactions between SEP4 and SOC1/ FUL were detected in the nuclei of the living tobacco cells, suggesting that *SEP4* may regulate its downstream genes together with *SOC1* and/or *FUL* (Figure 17C).

Previous study suggested that although *SOC1* is expressed throughout the vegetative seedlings, it mainly functions in the shoot apical meristem to promote flowering (Searle et al., 2006). Examination of the *SEP4* expression pattern indicates that *SEP4* is also expressed throughout the vegetative seedlings including leaves and the shoot apical meristems. It remains unclear whether *SEP4* promotes flowering mainly in the meristem like *SOC1* does. Therefore, to address this issue, two expression constructs were created to examine the spatial function of *SEP4* in flowering time control. An artificial miRNA was targeting against *SEP4* transcript were placed under the control of the phloem companion

cell-specific gene *SUC2* (*SUCROSE-PROTON SYMPORTER 2*) and the meristem-specific gene *KNAT1* (*KNOTTED-LIKE FROM ARABIDOPSIS THALIANA 1*) to induce its silencing, respectively (An et al., 2004; Jung et al., 2007). These two constructs, named *SUC2: amiR-SEP4* and *KNAT1: amiR-SEP4*, have already been transformed into the *soc1-2* single mutant to examine the spatial biological function of *SEP4*.

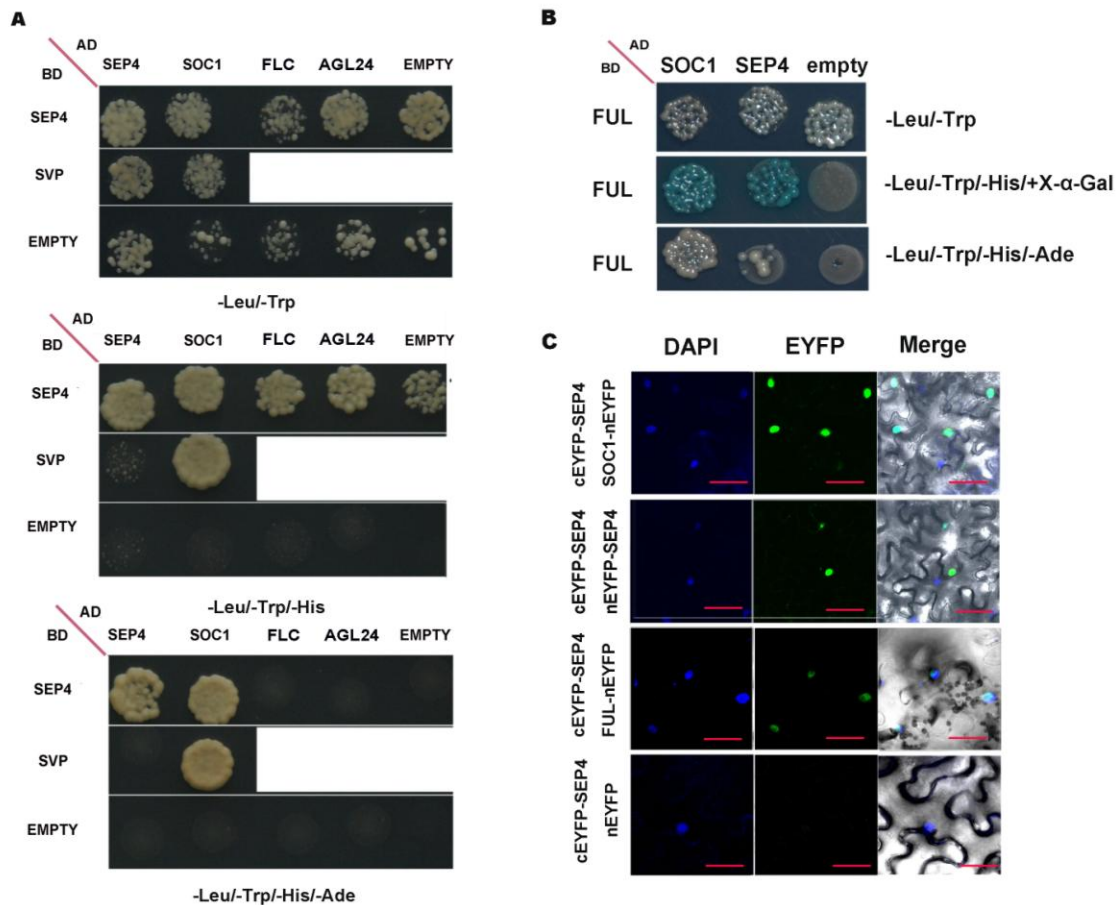


Figure 17. SEP4 Interacts with SOC1 and FUL.

(A) Yeast two-hybrid assay of the interaction between SEP4 and other flowering-time regulators. Transformed yeast cells were grown on SD/-Leu/-Trp, SD/-Leu/-Trp/-His and SD/-Leu/-Trp/-His/-Ade mediums (from top to bottom).

(B) Yeast two-hybrid assay of the interaction among FUL, SEP4 and SOC1. Transformed yeast cells were grown on SD/-Leu/-Trp, SD/-Leu/-Trp/-His/+ X- α -Gal and SD/-Leu/-Trp/-His/-Ade mediums (from top to bottom).

(C) BiFC analysis of the interaction between SEP4 and itself, SOC1 and FUL. DAPI, fluorescence of 4'6-diamidino-2-phenylindole; Merge, merge of EYFP and DAPI. Bars=20 μ m.

3.9 Putative interacting partners of SEP4 explored by yeast two-hybrid screening

To gain more insights on how *SEP4* regulates flowering time, a yeast-two hybrid screening was performed to identify proteins interacting with SEP4. The full-length SEP4 protein was fused to the Gal4 DNA-binding domain (BD-SEP4), and the libraries of prey proteins were fused to the Gal4 activation domain (AD). We used the Matchmaker Gold Yeast-Two Hybrid System to perform this screening. The mating efficiency was 2.4%, which fell within the recommend mating efficiency range (2% -5%). There were approximately 1 million diploids screened on the selection medium, from which about 2,000 surviving colonies were picked up and transferred to the TDO/X- α -Gal plates for further selection. Subsequently, about 400 colonies were picked up based on the intensity of blue color compared to the positive control (interaction between BD-SEP4 and AD-SOC1). Next, the yeast colony PCR was performed to amplify the library sequences, which finally yielded partial coding sequences of 163 genes. There are 35 transcriptional factors, 47 enzymes, 15 DNA/RNA binding proteins, 45 structure related proteins, 7 ribosomal proteins, and 14 unknown proteins (Figure 18A). Among all these candidates, there are 36 genes which appeared at least twice selected for further study.

Two candidates were chosen for further verifications via testing the interaction between full-length proteins and SEP4. One is WUSCHEL-RELATED HOMEODOMAIN 13 (WOX13), which has also been found among the list of 202 genes upregulated in the shoot apical meristem during floral induction (Torti et al., 2012). Loss of function of *WOX13* shows early flowering phenotype (Deveaux et al., 2008). Another one is INHIBITOR OF GROWTH 1 (ING1), which is a member of the ING family consisting of nuclear-localized PhD domain containing homeodomain proteins that bind to di- and tri-

methyated H3K4 (Lee et al., 2009). The yeast-two hybridization result demonstrated that both the full-length proteins WOX13 and ING1 could interacted with SEP4 (Figure 18B). Such interactions will be further confirmed by BiFC, *in vitro* glutathione S-transferase (GST) pull-down and Co-immunoprecipitation (Co-IP).

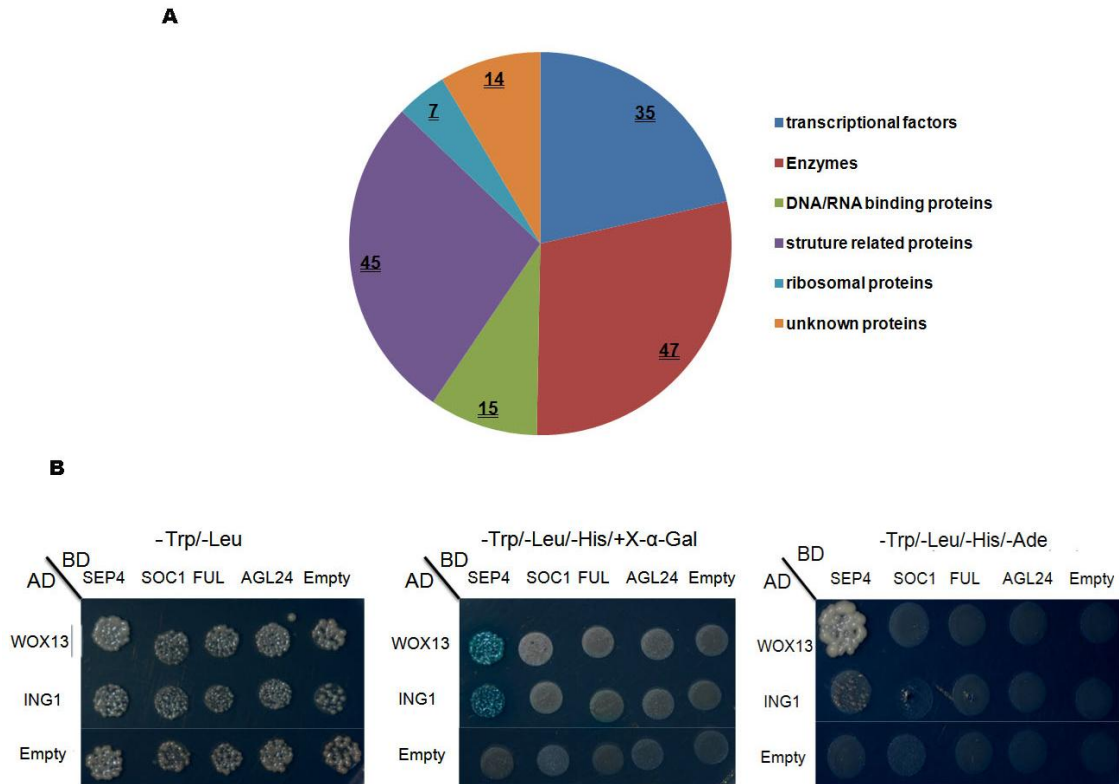


Figure 18. Putative interacting proteins of SEP4 selected by yeast-two hybrid screening.

(A) Pie chart shows the distribution of different proteins selective by yeast-two hybrid screening with BD-SEP4. The numbers of proteins in each group are shown.

(B) Yeast two-hybrid assay of the interactions between WOX13 and ING1 with SEP4 and other MADS-box proteins. Transformed yeast cells were grown on SD/-Leu/-Trp, SD/-Leu/-Trp/-His/+ X-α-Gal and SD/-Leu/-Trp/-His/-Ade mediums (from left to right)

CHAPTER 4

DISCUSSION

Chapter 4: Discussion

Flowering time of *Arabidopsis* is precisely regulated by multiple genetic pathways in response to various environmental and endogenous cues. The complex regulatory network is composed of a number of flowering time regulators including a group of MADS-box transcription factors, which contribute to determine the switch from vegetative shoot apical meristems to inflorescence meristems. Among these MADS-box regulators, *SOC1* serves as an important integrator functioning together with *FT* and *LFY* to activate the floral meristem identity genes to initiate flowering (Blazquez and Weigel, 2000; Parcy, 2005; Simpson and Dean, 2002). *SOC1* is mainly expressed in the SAM and developing leaves and integrates the signals perceived by the photoperiod pathway, autonomous pathway, vernalization pathway and GA pathway (Borner et al., 2000; Lee et al., 2000; Moon et al., 2003). In this study, we have identified another MADS-box gene, *SEP4*, as a flowering activator playing redundant functions with *SOC1*. Findings in this project will not only shed more light on the network that *SOC1* is involved in but also give us more leads about the dedicated and fine-tuned regulation mechanism of plant development.

SEP4 is firstly identified as an E-class organ identity gene specifying floral organs with other three homeotic genes, *SEP1*, *SEP2* and *SEP3* (Ditta et al., 2004). Furthermore, *SEP4* also contributes to maintain the floral meristem identity with *SOC1*, *AGL24* and *SVP* by repressing *TFL1* expression (Liu et al., 2013). In our study, we focus on the function of *SEP4* as a flowering time regulator. The bioinformatic analysis indicates the high similarity among *SEP4* and other *SEP* proteins in the conserved MADS-box domain and

K-domain, whereas the C-terminal regions are distinct (Figure 2A). The Glutamine-rich region in *SEP4* implies that it can directly serve as a transcriptional activator. In addition, 4 potential phosphorylation (R/KXXS/T) sites, enable *SEP4* to be phosphorylated (Figure 2B).

Although the loss of function mutant of *SEP4*, *sep4-1*, didn't show any distinguished flowering phenotype compared with wild-type, the overexpression lines flowered about 3 rosette leaves earlier than wild-type plants (Figure 3). These phenotypes may be due to the redundant function of *SEP4* with other genes as its function in floral organ identification. Furthermore, based on the results of the quantitative real-time PCR and GUS staining analysis, *SEP4* was mainly expressed in the developing leaves and stems, and the expression levels increased over the developmental stages, which is similar as *SOC1*. All of the findings above imply that *SEP4* could be involved in promoting flowering. To further characterize the specific expression patterns of *SEP4*, we have prepared a native *pSEP4::GFP-SEP4* construct harboring the 4.6 kb upstream sequence from the start codon, and *GFP* sequence inserted before the coding region of *SEP4* (Figure 19A). This construct has been transformed into the *soc1-2 sep4-1* double mutant successfully and the GFP-*SEP4* signal could be observed in the central region and vascular tissues of the shoot apex (Figure 19B). This transgenic line will be used for further study when we get the stable lines. In addition, RNA *in situ* hybridization experiment will be performed to examine the expression of *SEP4* in the shoot apical meristem during the floral transition.

In order to further understand how *SEP4* responds to the various flowering signals to regulate flowering time, we examined the expression of *SEP4* in different environmental conditions and flowering mutants. Our results revealed that *SEP4* is regulated by the au-

tonomous and photoperiod pathway, but not by the GA and vernalization pathway. Moreover, the circadian clock also had some effect on the regulation of *SEP4* expression.

The genetic data from the different combinations of *sep4-1* and other flowering time mutants showed that *sep4-1* could significantly enhance the late-flowering phenotype of *soc1-2* with about 7 more rosette leaves late. This finding is coincided with our proposal that *SEP4* may play a redundant function with *SOC1*, and the absence of *SOC1* leads to the prominent role of *SEP4* in regulating flowering time. We would like to further investigate how *SEP4* functions as an “alternative player”, therefore, we chose *soc1-2 sep4-1* mutant rather than *sep4-1* single mutants as the mainly research material.

In our study, among a lot of the key genes affected by the autonomous and photoperiod pathway, the expressions of *FT* and two of its repressors, *TEM1* and *TEM2* were significantly changed in the *soc1-2 sep4-1* double mutant compared with that in the *soc1-2* single mutant. Because the cDNA sequences of *TEM1* and *TEM2* show high similarity (Castillejo and Pelaz, 2008), we have been preparing an artificial microRNA construct to knock down these two genes together in *soc1-2 sep4-1* double mutant, then we will check whether the late flowering phenotype could be rescued. To further verify it, we have also generated an inducible line of *XVE:SEP4*, in which the transcription of *SEP4* can be activated by hormone treatment, in the *soc1-2 sep4-1* double mutant backgrounds. With such inducible line, the expression levels of *FT*, *TEM1* and *TEM2* could be examined in a time-course experiment. Furthermore, the results of ChIP (Chromatin Immunoprecipitation) experiment with *SEP4* antibody suggested that *SEP4* could bind to the same CArG-box motif in the promoter region of *TEM1* as *SOC1* when *SOC1* is missing (Figure 16) (Tao et al., 2012). In addition, a *gSEP4:4HA* construct with 2.6k promoter

region and the whole coding region of *SEP4* fused with 4HA tag has been successfully transferred into *soc1-2 sep4-1* mutants. This transgenic line will be used for the further analyzing target genes directly regulated by both *SOC1* and *SEP4*. And for further elucidate the relationship between *SOC1* and *SEP4*, the binding of SEP4 in wild type plants will also be tested by ChIP assay to explore the functions of *SEP4* with or without *SOC1* in flowering time regulation.

As a MIKC-type protein, SEP4 is supposed to function in regulating flowering time as a dimer or tetrameric complex with other MADS-box proteins as it regulates floral organ development and flower meristem identity (Kaufmann et al., 2005; Theissen, 2001; Theissen and Saedler, 2001). In our study, we found that SEP4 could interact with itself, SOC1 and FUL *in vitro* (Figure 17). The genetic interaction between *SOC1* and *SEP4*, and the *in planta* protein interaction between the two proteins, suggest that SEP4 might form a protein complex with SOC1 to promote flowering. And the *gSEP4:4HA* transgenic line will be used to investigate whether SEP4 can interact with SOC1 *in vivo* with Co-IP. Furthermore, FUL has been shown as a partner of SOC1 in regulating flowering time and meristem determinacy (Melzer et al., 2008). Considering *sep4-1 ful-7* double mutants shows the same flowering time as *ful-7* single mutant rather than later flowering time, we propose that both of them are interacting partners of SOC1, while they are not the only two partners. Therefore, the yeast-two screening with SEP4 could also give us more hints about the interacting partners of SOC1 and SEP4.

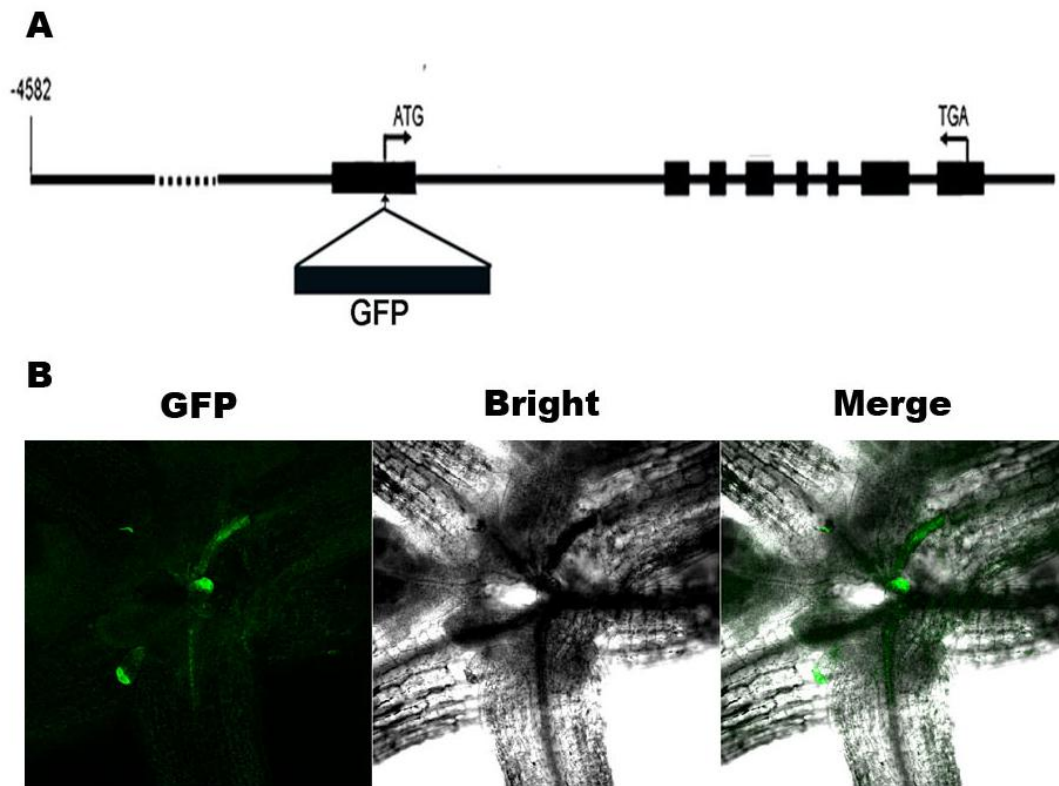


Figure 19. *In vivo* expression of SEP4 fusion protein.

(A) Schematic diagram shows the *GFP* insertion site in *SEP4* genomic regions. Exons and UTR regions are represented by black boxes, while introns, upstream regions are represented by black lines. Bent arrows denote translational start site and stop codon.

(B) An overview of the shoot apex in 9-days old *pSEP4:GFP-SEP4 soc1-2 sep4-l* transgenic lines. GFP-SEP4 signals were detected in the central region of the shoot apex.

CHAPTER 5

CONCLUSION

Chapter 5: Conclusion

In order to maximize the reproductive success, the switch from vegetative to reproductive growth of *Arabidopsis* is precisely regulated by a complex regulatory network. A group of MADS-box genes contribute a lot to regulating flowering time, among which *SOC1* is the floral integrator that converges the signals perceived by several genetic pathways. In this study, we find out another MADS-box gene, *SEP4*, promoting flowering as a redundant partner of *SOC1*.

Firstly, we found that except the highly conserved MADS-box domain and K-domain, *SEP4* contains extra Glutamine-rich regions and 4 potential phosphorylation (R/KXXS/T) sites. We found that the overexpression of *SEP4* caused early flowering, although *sep4-1* didn't show any distinguishable phenotype compared with wild-type. And the real time quantitative PCR and Gus staining results showed that *SEP4* was mainly expressed in the developing leaves and stems. Furthermore, the expression levels increased over the developmental ages. The above results suggested that *SEP4* could be a flowering activator.

Secondly, to further characterize the function of *SEP4* in regulating flowering time, the expression analysis revealed that *SEP4* was regulated by the autonomous and photoperiod pathway, but not by the GA and vernalization pathway. And *SEP4* expression was influenced by the circadian clock. We also found that *sep4-1* could significantly enhance the late-flowering phenotype of *soc1-2*, suggesting that *SEP4* may play a redundant function with *SOC1* in regulating flowering time. Therefore, *soc1-2 sep4-1* mutant rather than *sep4-1* single mutant was used as the main genetic material for further studies.

Thirdly, we have explored the putative downstream targets of *SEP4*. And we found the

expressions of *FT* and two of its repressors, *TEM1* and *TEM2* were significantly changed in the *soc1-2 sep4-1* double mutant compared with *soc1-2* single mutant. The upregulation of *FT* and downregulation of *TEM1* were further confirmed by the Gus staining experiments. In addition, ChIP (Chromatin Immunoprecipitation) assay suggested that SEP4 could bind to the same CArG-box motif in the 5'promoter region of *TEM1* as SOC1 did.

Last but not the least, in order to investigate the interaction partners of SEP4, we first found that among the MADS-box proteins involved in flowering time regulation, SEP4 itself, SOC1 and FUL could interact with SEP4 *in vitro*. Furthermore, we also performed the yeast-two screening with SEP4 to explore more candidates as the interaction partners of SEP4 and SOC1.

References

- An, H., Roussot, C., Suarez-Lopez, P., Corbesier, L., Vincent, C., Pineiro, M., Hepworth, S., Mouradov, A., Justin, S., Turnbull, C. et al.** (2004). CONSTANS acts in the phloem to regulate a systemic signal that induces photoperiodic flowering of *Arabidopsis*. *Development* **131**, 3615-26.
- Baldev, B. and Lang, A.** (1965). Control of flower formation by growth retardants and gibberellin in *Samolus parviflorus*, a long-day plant. *American Journal of Botany* **52**, 408-417.
- Bernier, G.** (1988). The control of floral evocation and morphogenesis. *Annual review of Plant Physiology and Plant Molecular Biology* **39**, 175-219.
- Blazquez, M. A. and Weigel, D.** (2000). Integration of floral inductive signals in *Arabidopsis*. *Nature* **404**, 889-892.
- Borner, R., Kampmann, G., Chandler, J., Gleissner, R., Wisman, E., Apel, K. and Melzer, S.** (2000). A MADS domain gene involved in the transition to flowering in *Arabidopsis*. *The Plant Journal* **24**, 591-599.
- Castillejo, C. and Pelaz, S.** (2008). The balance between CONSTANS and TEMPRANILLO activities determines FT expression to trigger flowering. *Current Biology* **18**, 1338-1343.
- Chien, J. C. and Sussex, I. M.** (1996). Differential regulation of trichome formation on the adaxial and abaxial leaf surfaces by gibberellins and photoperiod in *Arabidopsis thaliana* (L.) Heynh. *Plant Physiology* **111**, 1321-1328.
- Clough, S. J. and Bent, A. F.** (1998). Floral dip: a simplified method for *Agrobacterium*-mediated transformation of *Arabidopsis thaliana*. *The Plant Journal* **16**, 735-743.

- Coen, E. S. and Meyerowitz, E. M.** (1991). The war of the whorls: genetic interactions controlling flower development. *Nature* **353**, 31-37.
- Deveaux, Y., Toffano-Nioche, C., Claisse, G., Thareau, V., Morin, H., Laufs, P., Moreau, H., Kreis, M. and Lecharny, A.** (2008). Genes of the most conserved WOX clade in plants affect root and flower development in Arabidopsis. *BMC Evolutionary Biology* **8**, 291.
- Dill, A., Jung, H. S. and Sun, T.** (2001). The DELLA motif is essential for gibberellin-induced degradation of RGA. *Proceedings of the National Academy of Sciences of the United States of America* **98**, 14162–14167.
- Ditta, G., Pinyopich, A., Robles, P., Pelaz, S. and Yanofsky, M. F.** (2004). The SEP4 gene of Arabidopsis thaliana functions in floral organ and meristem identity. *Current Biology* **14**, 1935-1940.
- Dunlap, J. C.** (1996). Genetic and molecular analysis of circadian rhythms. *Annual Review of Genetics* **30**, 579-601.
- Fornara, F., de Montaigu, A. and Coupland, G.** (2010). SnapShot: control of flowering in Arabidopsis. *Cell* **141**, 550-550.
- Fosket, D. E.** (1994). Plant growth and development: a molecular approach. *Academic Press Inc.*
- Hamada, S., Onouchi, H., Tanaka, H., Kudo, M., Liu, Y. G., Shibata, D., Machida, C. and Machida, Y.** (2000). Mutations in the WUSCHEL gene of Arabidopsis thaliana result in the development of shoots without juvenile leaves. *The Plant Journal* **24**, 91-101.
- Huang, H., Tudor, M., Weiss, C. A., Hu, Y. and Ma, H.** (1995). The Arabidopsis MADS-box gene AGL3 is widely expressed and encodes a sequence-specific DNA-

binding protein. *Plant Molecular Biology* **28**, 549-567.

Jung, J.-H., Ju, Y., Seo, P. J., Lee, J.-H. and Park, C.-M. (2012). The SOC1-SPL module integrates photoperiod and gibberellic acid signals to control flowering time in *Arabidopsis*. *The Plant Journal* **69**, 577-588.

Jung, J. H., Seo, Y. H., Seo, P. J., Reyes, J. L., Yun, J., Chua, N. H. and Park, C. M. (2007). The GIGANTEA-regulated microRNA172 mediates photoperiodic flowering independent of CONSTANS in *Arabidopsis*. *The Plant Cell* **19**, 2736-2748.

Kagaya, Y., Ohmiya, K. and Hattori, T. (1999). RAV1, a novel DNA-binding protein, binds to bipartite recognition sequence through two distinct DNA-binding domains uniquely found in higher plants. *Nucleic Acids Research* **27**, 470-478.

Kaufmann, K., Melzer, R. and Theissen, G. (2005). MIKC-type MADS-domain proteins: structural modularity, protein interactions and network evolution in land plants. *Gene* **347**, 183-198.

Kay, S. A. and Millar, A. J. (1995). New models in vogue for circadian clocks. *Cell* **83**, 361.

Kobayashi, Y. and Weigel, D. (2007). Move on up, it's time for change—mobile signals controlling photoperiod-dependent flowering. *Genes & Development* **21**, 2371-2384.

Koornneef, M., Cone, J., Dekens, R., O'Herne-Robers, E., Spruit, C. and Kendrick, R. (1985). Photomorphogenic responses of long hypocotyl mutants of tomato. *Journal of Plant Physiology* **120**, 153-165.

Koornneef, M., Hanhart, C. and Veen, J. H. (1991). A genetic and physiological analysis of late flowering mutants in *Arabidopsis thaliana*. *Molecular and General Genetics* **229**, 57-66.

- Lee, H., Suh, S. S., Park, E., Cho, E., Ahn, J. H., Kim, S. G., Lee, J. S., Kwon, Y. M. and Lee, I.** (2000). The AGAMOUS-LIKE 20 MADS domain protein integrates floral inductive pathways in Arabidopsis. *Genes & Development* **14**, 2366-2376.
- Lee, W. Y., Lee, D., Chung, W. I. and Kwon, C. S.** (2009). Arabidopsis ING and Atfin1-like protein families localize to the nucleus and bind to H3K4me3/2 via plant homeodomain fingers. *The Plant Journal* **58**, 511-524.
- Li, D., Liu, C., Shen, L., Wu, Y., Chen, H., Robertson, M., Helliwell, C. A., Ito, T., Meyerowitz, E. and Yu, H.** (2008). A repressor complex governs the integration of flowering signals in Arabidopsis. *Developmental Cell* **15**, 110-120.
- Litt, A. and Kramer, E. M.** (2010). The ABC model and the diversification of floral organ identity, *Seminars in Cell & Developmental Biology* **21**, 129-137:
- Liu, C., Chen, H., Er, H. L., Soo, H. M., Kumar, P. P., Han, J. H., Liou, Y. C. and Yu, H.** (2008). Direct interaction of AGL24 and SOC1 integrates flowering signals in Arabidopsis. *Development* **135**, 1481-1491.
- Liu, C., Teo, Z. W. N., Bi, Y., Song, S., Xi, W., Yang, X., Yin, Z. and Yu, H.** (2013). A conserved genetic pathway determines inflorescence architecture in Arabidopsis and Rice. *Developmental Cell* **24**, 612-622.
- Mathieu, J., Yant, L. J., Murdter, F., Kuttner, F. and Schmid, M.** (2009). Repression of flowering by the miR172 target SMZ. *PLoS Biology* **7**, e1000148.
- Melzer, S., Lens, F., Gennen, J., Vanneste, S., Rohde, A. and Beeckman, T.** (2008). Flowering-time genes modulate meristem determinacy and growth form in Arabidopsis thaliana. *Nature Genetics* **40**, 1489-1492.
- Meyerowitz, E. M. and Somerville, C. R.** (1994). Arabidopsis. *Cold Spring Harbor*

Laboratory Print.

Michaels, S. D. and Amasino, R. M. (1999). FLOWERING LOCUS C encodes a novel MADS domain protein that acts as a repressor of flowering. *The Plant Cell* **11**, 949-956.

Michaels, S. D. and Amasino, R. M. (2001). Loss of FLOWERING LOCUS C activity eliminates the late-flowering phenotype of FRIGIDA and autonomous pathway mutations but not responsiveness to vernalization. *The Plant Cell* **13**, 935-942.

Moon, J., Suh, S. S., Lee, H., Choi, K. R., Hong, C. B., Paek, N. C., Kim, S. G. and Lee, I. (2003). The SOC1 MADS-box gene integrates vernalization and gibberellin signals for flowering in Arabidopsis. *The Plant Journal* **35**, 613-623.

Napp-Zinn, K. (1961). Vernalisation und verwandte Erscheinungen. *Handbuch der Pflanzenphysiologie* **16**, 24-75.

Napp-Zinn, K. and Atherton, J. (1987). Vernalization-environmental and genetic regulation. *Manipulation of Flowering*, 123-132.

Osnato, M., Castillejo, C., Matías-Hernández, L. and Pelaz, S. (2012). TEMPRANILLO genes link photoperiod and gibberellin pathways to control flowering in Arabidopsis. *Nature Communications* **3**, 808.

Parcy, F. (2005). Flowering: a time for integration. *The International Journal of Developmental Biology* **49**, 585-593.

Pelaz, S., Tapia-López, R., Alvarez-Buylla, E. R. and Yanofsky, M. F. (2001). Conversion of leaves into petals in Arabidopsis. *Current Biology* **11**, 182-184.

Putterill, J., Laurie, R. and Macknight, R. (2004). It's time to flower: the genetic control of flowering time. *Bioessays* **26**, 363-373.

Riechmann, J. L., Krizek, B. A. and Meyerowitz, E. M. (1996). Dimerization

specificity of Arabidopsis MADS domain homeotic proteins APETALA1, APETALA3, PISTILLATA, and AGAMOUS. *Proceedings of the National Academy of Sciences of the United States of America* **93**, 4793–4798

Samach, A., Onouchi, H., Gold, S. E., Ditta, G. S., Schwarz-Sommer, Z., Yanofsky, M. F. and Coupland, G. (2000). Distinct roles of CONSTANS target genes in reproductive development of Arabidopsis. *Science* **288**, 1613-1616.

Sawa, M. and Kay, S. A. (2011). GIGANTEA directly activates Flowering Locus T in Arabidopsis thaliana. *Proceedings of the National Academy of Sciences of the United States of America* **108**, 11698-11703.

Searle, I. (2006). The transcription factor FLC confers a flowering response to vernalization by repressing meristem competence and systemic signaling in Arabidopsis. *Genes & Development* **20**, 898-912.

Shannon, S. and Meeks-Wagner, D. R. (1991). A mutation in the Arabidopsis TFL1 gene affects inflorescence meristem development. *The Plant Cell* **3**, 877-892.

Sieburth, L. E. and Meyerowitz, E. M. (1997). Molecular dissection of the AGAMOUS control region shows that cis elements for spatial regulation are located intragenically. *The Plant Cell* **9**, 355-65.

Simon, R., Igeño, M. I. and Coupland, G. (1996). Activation of floral meristem identity genes in Arabidopsis. *Nature* **384**, 59-62

Simpson, G. G. and Dean, C. (2002). Arabidopsis, the Rosetta stone of flowering time? *Science* **296**, 285-289.

Sparkes, I. A., Runions, J., Kearns, A. and Hawes, C. (2006). Rapid, transient expression of fluorescent fusion proteins in tobacco plants and generation of stably

- transformed plants. *Nature Protocols* **1**, 2019-2025.
- Srikanth, A. and Schmid, M.** (2011). Regulation of flowering time: all roads lead to Rome. *Cellular and Molecular Life Sciences* **68**, 2013-2037.
- Suárez-López, P., Wheatley, K., Robson, F., Onouchi, H., Valverde, F. and Coupland, G.** (2001). CONSTANS mediates between the circadian clock and the control of flowering in Arabidopsis. *Nature* **410**, 1116-1120.
- Sun, T. and Kamiya, Y.** (1994). The Arabidopsis GA1 locus encodes the cyclase entkaurene synthetase A of gibberellin biosynthesis. *The Plant Cell* **6**, 1509-1518.
- Sung, S. and Amasino, R. M.** (2004a). Vernalization and epigenetics: how plants remember winter. *Current Opinion in Plant Biology* **7**, 4-10.
- Sung, S. and Amasino, R. M.** (2004b). Vernalization in Arabidopsis thaliana is mediated by the PHD finger protein VIN3. *Nature* **427**, 159-164.
- Swain, S. M. and Olszewski, N. E.** (1996). Genetic analysis of gibberellin signal transduction. *Plant Physiology* **112**, 11.
- Swaminathan, K., Peterson, K. and Jack, T.** (2008). The plant B3 superfamily. *Trends in Plant Science* **13**, 647-655.
- Tao, Z., Shen, L., Liu, C., Liu, L., Yan, Y. and Yu, H.** (2012). Genome-wide identification of SOC1 and SVP targets during the floral transition in Arabidopsis. *The Plant Journal* **70**, 549-561.
- Telfer, A., Bollman, K. M. and Poethig, R. S.** (1997). Phase change and the regulation of trichome distribution in *Arabidopsis thaliana*. *Development* **124**, 645-654.
- Theissen, G.** (2001). Development of floral organ identity: stories from the MADS house. *Current Opinion in Plant Biology* **4**, 75-85.

- Theissen, G., Kim, J. T. and Saedler, H.** (1996). Classification and phylogeny of the MADS-box multigene family suggest defined roles of MADS-box gene subfamilies in the morphological evolution of eukaryotes. *Journal of Molecular Evolution* **43**, 484-516.
- Theissen, G. and Saedler, H.** (2001). Plant biology. Floral quartets. *Nature* **409**, 469-471.
- Torti, S., Fornara, F., Vincent, C., Andres, F., Nordstrom, K., Gobel, U., Knoll, D., Schoof, H. and Coupland, G.** (2012). Analysis of the Arabidopsis shoot meristem transcriptome during floral transition identifies distinct regulatory patterns and a leucine-rich repeat protein that promotes flowering. *The Plant Cell* **24**, 444-462.
- Turck, F., Fornara, F. and Coupland, G.** (2008). Regulation and identity of florigen: FLOWERING LOCUS T moves center stage. *Annual Review of Plant Biology* **59**, 573-594.
- Wang, J. W., Czech, B. and Weigel, D.** (2009). miR156-Regulated SPL transcription factors define an endogenous flowering pathway in Arabidopsis thaliana. *Cell* **138**, 738-749.
- Wigge, P. A., Kim, M. C., Jaeger, K. E., Busch, W., Schmid, M., Lohmann, J. U. and Weigel, D.** (2005). Integration of spatial and temporal information during floral induction in Arabidopsis. *Science* **309**, 1056-1059.
- Wilson, R. N., Heckman, J. W. and Somerville, C. R.** (1992). Gibberellin is required for flowering in Arabidopsis thaliana under short days. *Plant Physiology* **100**, 403-408.
- Wu, G., Park, M. Y., Conway, S. R., Wang, J. W., Weigel, D. and Poethig, R. S.** (2009). The sequential action of miR156 and miR172 regulates developmental timing in Arabidopsis. *Cell* **138**, 750-759.
- Yoo, S. K.** (2005). CONSTANS activates SUPPRESSOR OF OVEREXPRESSION OF

CONSTANS 1 through FLOWERING LOCUS T to promote flowering in Arabidopsis.
Plant Physiology **139**, 770-778.